PREPARATION OF HYDROPHILIC NANOCRYSTALS USING LIPOIC ACID BASED SYNTHETIC LIGANDS

By

SHUO YANG

A THESIS PRESENTED TO THE GRADUATE SCHOOL
OF THE UNIVERSITY OF FLORIDA IN PARTIAL FULFILLMENT
OF THE REQUIREMENTS FOR THE DEGREE OF
MASTER OF SCIENCE

UNIVERSITY OF FLORIDA

2008

To my wife and my parents

ACKNOWLEDGMENTS

First, I would like to thank my wife and my parents. It is their unconditional love and supports that helped me get to where I am today.

I want to thank my advisor, Dr. Y. Charles Cao, for his guidance and support. I appreciate all of his help and suggestions on my research and my life. I also want to thank Huimeng Wu for all the help in the lab and Dr. Jiaqi Zhuang for the helpful discussions. Additionally, I want to say thank you to all the Cao group members for their help and friendship.

Finally, I would like to express my appreciation to Dr. Ben Smith for helping me through my difficult times.

TABLE OF CONTENTS

page

LIST OF FIGURES

Abstract of Thesis Presented to the Graduate School
of the University of Florida in Partial Fulfillment of the
Requirements for the Degree of Master of Science

PREPARATION OF HYDROPHILIC NANOCRYSTALS USING LIPOIC ACID BASED SYNTHETIC LIGANDS

By

Shuo Yang

August 2008

Chair: Y. Charles Cao
Major: Chemistry

Over the past several decades, nanocrystals have generated a tremendous amount of interest. They are employed in biological and medical studies for sensing, labeling, optical imaging, and drug delivery. High-quality colloidal nanocrystals are normally synthesized in organic phase with the presence of strongly coordinating hydrophobic organic ligands. However, using nanocrystals in biological system means that these nanomaterials have to be well dispersed and stable in aqueous solution. To meet the criteria, surface functionalization is needed to tailor the solubility and biocompatibility of nanocrystals and preserve their desired properties.

To prepare water-soluble nanocrystals, there are generally two approaches. The first one is ligand exchange via coordinate bonding and the other one makes use of hydrophobic van der Waals interaction between amphiphilic polymers and original surface ligands. Considering both advantages and disadvantages of the above two approaches, a new class of dual-interaction ligand was developed by using Tween20 and lipoic acid. DHLA-Tween20 ligand modified nanocrystals are more stable than the other water-soluble nanoparticles functionalized with either ligand exchange or polymer encapsulation approach. By having both coordinate bonding and hydrophobic molecular interaction, this new ligand renders modified hydrophilic nanocrystals superior stability and keeps the particle size relatively small. This new surface modification

approach can be used to nanocrystal with different compositions and will help develop more biomedical applications using nanomaterials.

Another lipoic acid based ligand was synthesized for gold nanoparticle functionalization. It is expected to develop a platform for simple and rapid phosphatase detection by incorporating phosphate group into synthetic ligand structure. Although the stability is relatively low, the hydrophilic gold nanoparticles were obtained through surface modification using the phosphate group-containing ligand. Further work is needed to produce more stable water-soluble Au nanoparticles and test their efficiency in phosphatase detection assay.

CHAPTER 1
PREPARATION OF HYDROPHILIC NANOCRYSTALS

1.1 Introduction

Over the past several decades, nanocrystals have generated a tremendous amount of interest. This has been motivated by a desire to reach a fundamental understanding of their unique size-dependent optical, electronic, magnetic, and chemical properties and by the potential applications involving the use of these materials. The applications range from electrical devices to biological and medical research.[1-15] Nanocrystals are crystalline clusters of a few hundred to a few thousand atoms with sizes of a few nanometers. Although more complex than individual atoms, their properties are different from bulk crystals.[16,17] Due to their small size, much of their chemical and physical properties are dominated by their surfaces and not by their bulk volume. Nanocrystals can be synthesized from metallic materials and semiconductor materials. Colloidal nanocrystals are the ones dispersed in a solvent and stabilized in a way that prevents aggregation.

Nowadays, colloidal nanocrystals are employed in biological and medical studies for sensing, labeling, optical imaging, and drug delivery. High-quality colloidal nanocrystals are normally synthesized in an organic phase with the presence of strongly coordinating hydrophobic organic ligands, such as trioctylphosphine (TOP) or trioctylphosphine oxide (TOPO).[18-20] However, using nanocrystals in biological system means that these nanomaterials have to be well dispersed and stable in aqueous solution. To meet the criteria, surface functionalization is needed to tailor the solubility of nanocrystals in different solvents and preserve their desired properties.

1.2 General Methods of Nanocrystal Surface Modification

High-quality metal and semiconductor nanomaterials are often prepared from organometallic precursors with surface-capping organic ligand.[1, 20-24] This capping ligand binds to the metal/semiconductor clusters, prevents aggregation of the particles into bulk material, and

controls the final dimensions of the nanoparticles. The commonly used organic ligands include trioctylphosphine (TOP), trioctylphosphine oxide (TOPO), oleic acid, and long chain alkyl-amines. The typical experiment setup of injection-based synthetic method is shown in Figure 1-1.

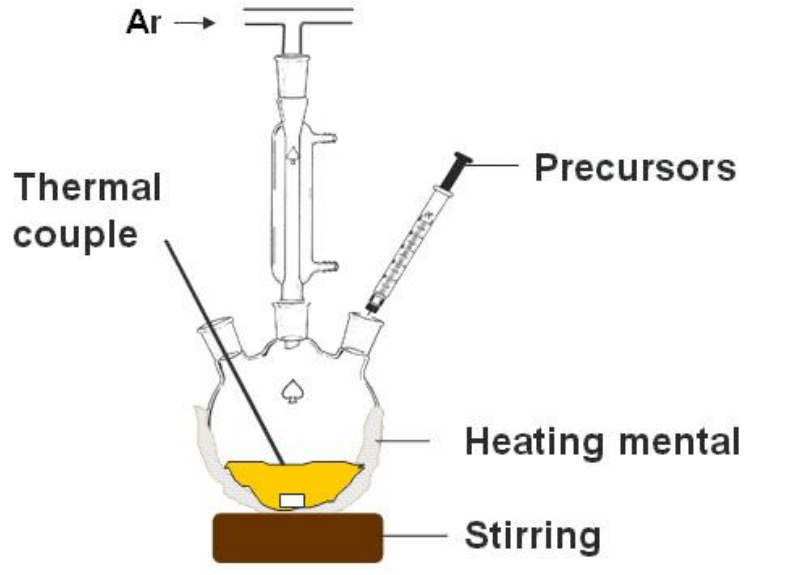

Figure 1-1. Typical experiment set-up of the injection-based method.

Since biological processes are typically situated in an aqueous environment, using these nanocrystals (quantum dots) in biological applications must somehow transform the surface coatings into hydrophilic materials. Ligand exchange process could be used to replace the original organic ligands with hydrophilic capping molecules. Another approach is to wrap the nanocrystals in an amphiphilic polymer whose hydrophobic ends interact with, but not replace, the organic coating on a nanocrystal. Also, silica encapsulation can be employed to prepare water-soluble and biocompatible nanocrystals as well (Figure 1-2).[25]

1.2.1 Ligand Exchange Method

Currently, high-quality nanocrystals are synthesized by "wet chemistry" procedures in organic phase in most cases. Organic capping of nanocrystals with surfactants can provide electron passivation and form a barrier against aggregation of crystalities. As a consequence, the

synthesized nanocrystals are hydrophobic. To obtain water-soluble particles, ligand exchange process was developed to replace the original surface coating molecules with hydrophilic ones. These bifunctional molecules are normally hydrophilic on one end and bind to nanocrystal surface with the other end. Functional groups such as thiols, dithiols, phosphines, and hydroxyl groups on dopamine, are involved.[15, 26-29]

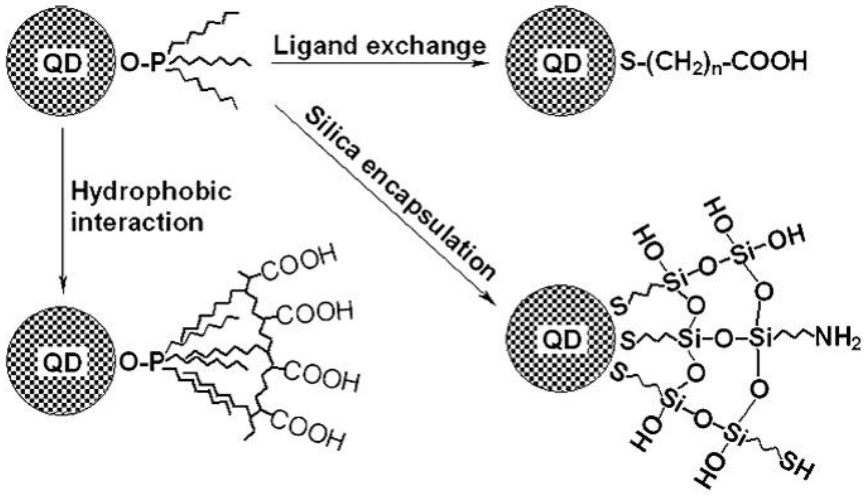

Figure 1-2. Quantum dot surface modification strategies.

In 1998, water-soluble mercaptoacetic acid modified CdSe/ZnS core-shell QD was reported by Warren Chan and Shuming Nie.[15] And these highly luminescent semiconductor quantum dots were covalently coupled to biomolecules via carboxylic acid functional group for use in ultrasensitive biological detection (Figure 1-3). In comparison with organic dye rhodamine R6G, this class of luminescent labels is 20 times as bright, 100 times as stable against photobleaching and one-third as wide in spectral line width. Also, these QD bioconjugates exhibited specific recognition and good sensitivity in immunoassay.

Later on, using ligand exchange method with various water-soluble bifunctional molecules to make hydrophilic and biocompatible nanocrystal became a very active area of research. Examples of some bi-functional ligands used are mercaptocarbonic acids [HS-(CH_2)n-COOH, n

= 1–15],[15, 23] dithiothreitol (DTT),[30] lipoic acid,[26] oligomeric phosphines,[31] peptides,[32] and cross-linked dendrons.[33] The general procedure of ligand exchange includes reacting the hydrophilic molecules with nanocrystals in organic phase for certain period of time, drying or evaporation of organic solvent, dissolution in water, and purification if necessary. Overall, the process is easy to handle and not time-consuming. The obtained nanocrystals normally have good distribution in water and can readily conjugated to biological molecules for further applications. However, there are certain drawbacks should be addressed. Ligand exchange inevitably alters the chemical and physical states of the nanocrystals surface atoms; thiol-based molecules (e.g. mercaptocarbonic acids) may form disulfides over time and come off from the surface and finally the nanocrystals aggregate and precipitate out of water; [23] the cross-linking of dendrons needs low nanoparticle concentration to avoid inter-particle reactions;[33] most of the achieved water-soluble nanoparticles are not stable under acidic or basic conditions or in solution containing certain concentration of salt, which is a common condition anticipated in biological applications.

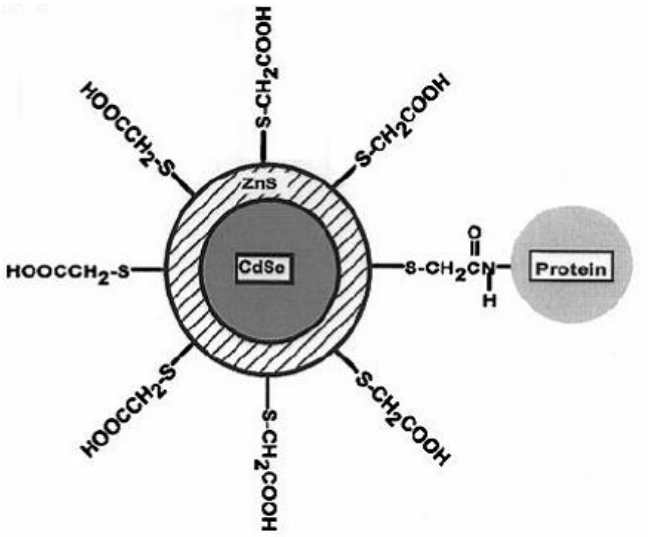

Figure 1-3. Schematic of a mercaptoacetic acid capped CdSe/ZnS QD coupled to a protein.

1.2.2 Polymer and Silica Encapsulation

Other than changing the original surface coating molecules, chemists developed methods to encapsulate the nanocrystals with polymers or in silica shell. In 2002, Benoit Dubertret and co-workers reported phospholipids micelle encapsulated CdSe/ZnS quantum dots and its application as fluorescent label for *in vivo* imaging (Figure 1-4).[34] They found that without any surface modifications, individual ZnS-overcoated CdSe QDs could be encapsulated in the hydrophobic core of a micelle composed of a mixture of n-poly (ethylene glycol) phosphatidylethanolamine (PEG-PE) and phosphatidylcholine (PC). This micelle structure delivers colloidal stability in water and reduces non-specific binding in complex mixture due to the presence of a dense layer of PEG polymers on the outer surface.

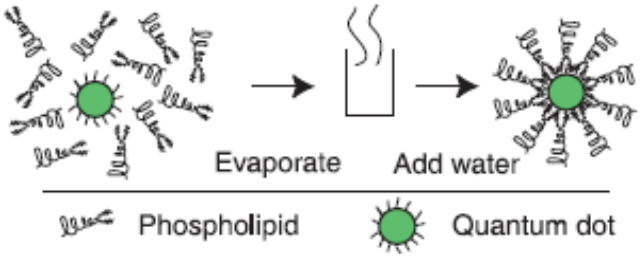

Figure 1-4. Schematic of single-QD encapsulation in a phospholipids micelle

Other examples of polymer encapsulation can be found in the publications contributed by the research groups of S. Nie, and V. Colvin.[3, 35] Nie group introduced the using of long chain length amphiphilic polymer to coat the surface of the nanocrystals (Figure 1-5).[3] This strategy of using amphiphilic polymers is generally superior to the ligand exchange on some aspects. Since there is no direct interaction with the particle surface atoms, the original optical properties of nanocrystals can be well preserved. And the polymer's large number of hydrophobic side chains strengthens the hydrophobic interaction to form stable water-soluble structures. Also, these amphiphilic polymers are generally commercially available with low prices and can be modified to achieve desired biocompatibility. However, this method normally produces water-soluble

nanocrystals with larger hydrodynamic diameters on the order of 30-40 nm which could be a potential problem for biological applications.

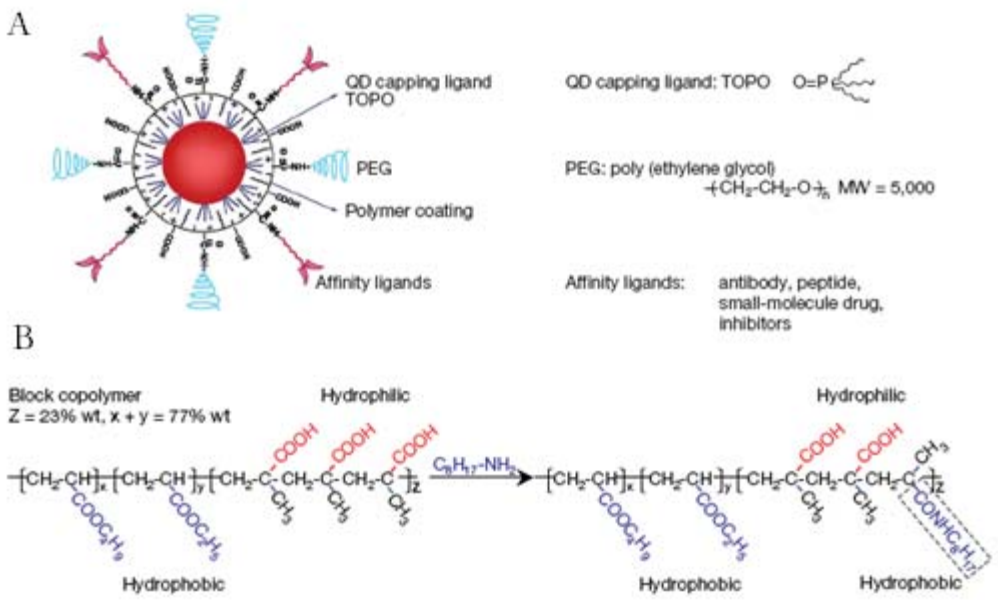

Figure 1-5. Schematic illustration of amphiphilic polymer coated QD. A) Structure of a bioconjugated multifunctional QD probe. B) Chemical structure of modified triblock copolymer used in QD surface coating.

Compared to ligand exchange and polymer coating, silica encapsulation will incorporate functional organosilicone molecules containing primary amine or thiol group into the shell and provide surface functionalities for biomedical applications.[14, 36-39] But with the crosslinked silica layer, the size of water-soluble nanocrystals prepared this way ranges from tens of nanometers to several micrometers. And the procedure is relatively complicated and laborious.

In essence, the preparation of water-soluble nanomaterials depends on two major approaches, coordinate bonding between particle surface atoms and appropriate functional groups and hydrophobic van der Waals interactions between original organic capping molecules and the hydrophobic branches of coating polymers.

1.3 Biomedical Applications of Water-Soluble Nanocrystals

For the last decade, nanocrystals, especially colloidal quantum dots, have been drawing great attention as a new class of powerful tool in biological and medical investigations. With their superior optical properties, water-soluble quantum dots are competent for the applications in cellular labeling, imaging, sensing and screening.

Before the emergence of quantum dots based assays, organic dyes are the primary fluorescent label for cellular imaging and bioassay detection. However, the intrinsic optical properties of organic fluorophores, which generally have broad absorption/emission profiles and low photobleaching thresholds, have limited their applications in long-term imaging and multiplex detection.[40] Compared with organic dye molecules, colloidal quantum dots have continuous excitation spectra and narrow emission, readily tunable luminescence, and high photobleaching thresholds.[12, 41-43]

The water-soluble quantum dots will be conjugated to biomolecules (DNAs, proteins) so that the resulting conjugates can combine both the spectroscopic characteristics of nanostructures and the biomolecular function of the surface-attached entities. Conjugation process for adding biocompatibility to quantum dots can be divided into three categories, (i) Use of EDC, 1-ethyl-3-(3-dimethylaminopropyl) carbodiimide, condensation to react carboxyl groups on the QD surface to amines; (ii) direct binding to the QD surface using thiolated peptides or polyhistidine (HIS) residues; and (iii) adsorption or noncovalent self-assembly using engineered proteins.[44]

1.3.1 Cellular Labeling

Cellular labeling is where QDs use has made the most progress and attracted the greatest interest. In a typical assay, the bioconjugated QDs will be transported into cell with different strategies.[45-47] They may include non-specific uptake by endocytosis; direct microinjection of nanolitre volumes; electroporation, which uses charge to physically deliver QDs through the

membrane; and mediated/targeted uptake using encapsulates QDs within lipid vesicles to facilitate entry into the cell. It has been proved that QDs can cross into cells and bind to their intended intracellular targets via specific recognition. Also, QDs can serve as useful markers for tracking cellular movement, differentiation and fate. Recent findings explicitly showed that QDs are not just useful alternatives to organic fluorophores in cell labeling. Their intrinsic optical properties make them unique in investigation of complex cellular processes, especially with their multicolor labeling capability.

1.3.2 In vivo and Deep Tissue Imaging

For imaging tissue with far red/near infrared excitation, quantum dots can be used to achieve deeper penetration in tissue compared to the available near-infrared dye molecules demonstrated by applying near-infrared emitting QDs (840–860 nm) to sentinel lymph-node mapping in cancer surgery of animals.[73] Due to their large two-photon cross-sectional efficiency with a two-photon fluorescence process 100–1,000× that of organic dyes, QDs are suitable for *in vivo* deep-tissue imaging using two-photon excitation at low intensities[48, 49]. In addition, QDs have been demonstrated to remain fluorescent in tissues *in vivo* for up to four months.[74] This property makes QDs excellent choice for tracking and visualizing cancer cells during metastasis.[3, 48] Conjugated with tumor-targeting antibodies, quantum dots can track cells *in vivo* over a long period of time without continuously sacrificing animals. Although QDs are certainly better choice than traditional dye molecules for these applications, without thorough toxicology studies, it is debatable that whether the QD probe is providing true *in vivo* physiology information.

CHAPTER 2
PREPARATION OF HYDROPHILIC NANOCRYSTALS USING DHLA-TWEEN20 LIGAND

2.1 Introduction

As discussed in last chapter, to date, most of the high-quality nanocrystals are synthesized in organic phase with the presence of various hydrophobic surface-capping ligands. These ligands help us keep the particles from aggregation and control the final dimensions of synthesized nanocrystals. Consequently, the synthetic nanocrystal does not possess the intrinsic solubility in aqueous solution.

To prepare water-soluble nanocrystals, surface modification is needed to deliver hydrophilicity. There are generally two approaches to modify particle surface for this purpose. The first one is known as ligand exchange.[15, 44, 50-52] A new organic ligand with hydrophilic group on one end and an anchor functional group on the other will be added to the nanocrystals organic solution. The anchor group, such as thiol or phosphine, has the ability to form coordinate bonding with the nanocrystal surface atom. Therefore, the new ligand will compete with the original ligands and partially remove them from the particle surface. Then the nanocrystal will be water-soluble because of the hydrophilic group on the other end of the substitute ligand. However, water-soluble particles prepared by this approach usually suffer from low stability and make them undesirable in *in vivo* imaging and tracking.

The other approach makes use of hydrophobic van der Waals interaction between, in most cases, amphiphilic polymers and original surface ligands.[35, 53-55] In aqueous solution, hydrophobic branches of polymer will interact with, but not remove, the original hydrophobic ligands on the surface. This interaction will encapsulate nanocrystal and form a shell-like structure to provide additional protection for the particle inside. The hydrophilic tails of amphiphilic polymer ligand make sure the modified nanocrystal is water-soluble. Although the

water-soluble nanocrystals made by this method are normally more stable than the ones went through ligand exchange process, the size of the particles is rather too large for some biomedical applications.

Considering both advantages and disadvantages of the above two approaches, we are going to develop a new kind of ligand which could produce stable water-soluble nanocrystals while keeping a relatively small size. Lipoic acid and Tween20 (polyethylene glycol sorbitan monolaurate) were chosen to synthesize the new ligand. Tween20, with 20 ethylene glycol units distributed among four branches (Figure 2-1), is often used in food industry as food additive because of its relative nontoxicity.[56] Also, it is widely used in bioassays, such as ELISA (enzyme-linked immunosorbent assay) and western blotting, [57, 58] to minimize nonspecific binding. These features make Tween20 a good candidate of coating nanocrsytal for biological applications. However, the interaction between Tween20's fatty acid chain and hydrophobic nanocrystal surface is rather too weak to stabilize particle in water. The bidentate structure in dihydrolipoic acid, reduced from lipoic acid, (Figure 2-2) can provide two thiol functional groups that make simultaneous capping attachment to two surface sites on the nanocrystal, theoretically resulting in more stable ligand/particle interactions. Therefore, we will modify Tween20 structure with lipoic acid in searching for a new class of ligand has both hydrophobic molecualr interaction and coordinate bonding with nanocrystals surface.

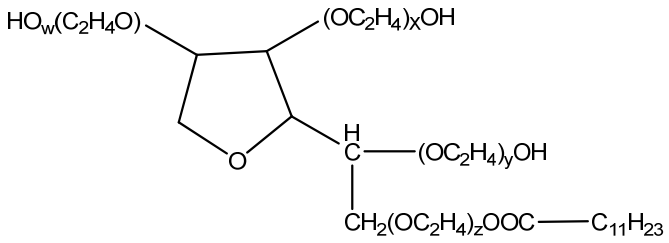

Figure 2-1. Structure of Tween20 (polyethylene glycol sorbitan monolaurate) (w+x+y+z=20)

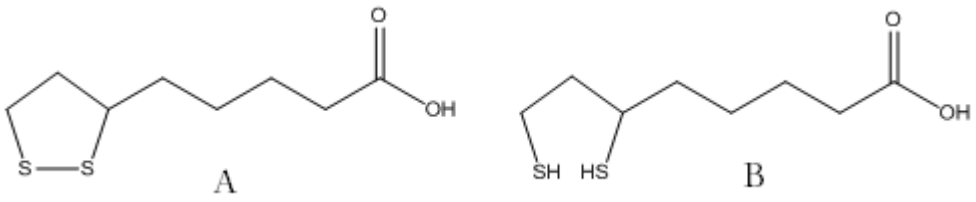

Figure 2-2. Structure of A) lipoic acid and B) dihydrolipoic acid

2.2 Experimental Section

2.2.1 Material

Dimethylaminopyridine (DMAP, 99%), N,N'-diisopropyl carbodiimide (DIPC, 99%), polyethylene glycol sorbitan monolaurate (Tween-20), sodium borohydride ($NaBH_4$, 97%), 1-dodecanethiol (97%), 1-octadecene (ODE, 90%), octadecylamine (ODA, 97%), p-toluenesulfonic acid monohydrate (98%), Rhodamine 6G (99%), and trioctylphosphine oxide (TOPO, 99%), were purchased from Sigma-Aldrich. Cadmium oxide (CdO, 99.998%), selenium (Se, 99.99%), dodecyl trimethylammonium bromide (DTAB, 97%) were purchased from Alfa Aesar. Nanopure water (18.2 MΩ·cm) was prepared by a Barnstead Nanopure Diamond system. All the other reagents and solvents were purchased from Fisher Scientific International Inc. All chemicals were used without further purification. CdSe/ZnS core-shell quantum dots were synthesized and provided by Ou Chen and Dr. Yongan Yang.

2.2.2 Instrumentation

NMR spectra were recorded using a Varian Mercury NMR Spectrometer (300 MHz). The samples were prepared by adding aliquots of products into a deuterated solvent ($CDCl_3$).

Absorption spectra of aliquots were collected by a Shimadzu UV-1700 UV-Visible Spectrophotometer. The wavelength and absorption of each aliquot were recorded.

Fluorescent spectra were measured using a Jobin Yvon Horiba Fluorolog-3 Model FL3-12 Spectrofluorometer. Room-temperature fluorescence QY of the CdSe/ZnS core/shell QDs was determined by using R6G as standard.

The nanoparticle aqueous solutions were filtered through a 0.22-μm MCE syringe filter (Fisher Scientific) first. The hydrodynamic sizes of nanocrystals were obtained from dynamic light scattering (DLS) (Brookhaven Instruments Corporation, Holtsville, NY) at 25 ^{o}C.

TEM measurements were performed on a JEOL 200CX operated at 200 kV. The specimens were prepared as follows: a particle solution (10 μL) was dropped onto a 200-mesh copper grid, and dried overnight at ambient conditions.

2.2.3 Experimental Procedures

2.2.3.1 Synthesis of 1-dodecanethiol-capped gold nanocrystals

Gold nanoparticles were synthesized according to the literature procedure.[59] In a typical synthesis, $AuCl_3$ (0.068 g) was dissolved in a DTAB solution (0.185 g of DTAB in 20 ml of toluene) with ultrasonication to form a dark orange solution. Then a freshly-prepared aqueous solution of $NaBH_4$ (75 μmol) was added dropwise to the solution with vigorous stirring. After 20 minutes, 1-dodecanethiol (1.6 ml) was added and the stirring was continued for 10 minutes. The nanoparticles were precipitated by adding ethanol, and the solid was re-dispersed in toluene (20 ml) in the presence of 1-dodecanethiol (1.6 ml) and refluxed for 30 minutes under nitrogen. The nanocrystals were precipitated from the reaction solution with ethanol (30 ml), isolated by centrifugation and re-dispersed in $CHCl_3$. The resulting nanoparticles have a diameter of 6.6 nm with a standard deviation of 7.0 %

2.2.3.2 Synthesis of dihydrolipoic acid (DHLA) functionalized Tween20

4-(N,N'-Dimethylamino)pyridinium-4-toluenesulfonate (DPTS) was prepared by mixing THF solutions of DMAP (2 M, 50 ml) and p-toluenesulfonic acid monohydrate (2 M, 50 ml) at room temperature with stirring. The resulting precipitate was filtered and dried under vacuum.

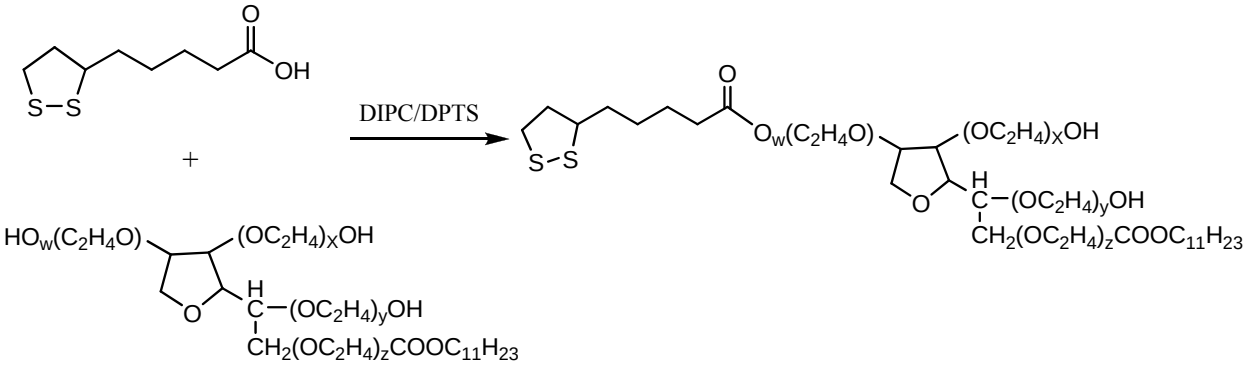

[5-(1,2-Dithiolan-3-yl)-1-oxopentyl]polyethylene glycol sorbitan monolaurate. Tween-20 (4.91 g, 4.0 mmol), lipoic acid (0.83 g, 4.0 mmol), and DPTS (1.37 g, 4.4 mmol) were mixed in CH_2Cl_2 (30 ml) and stirred for 10 minutes at room temperature. Then, DIPC (0.63 ml, 4.4 mmol) was added to the mixture. After being stirred at room temperature overnight, the precipitation was filtered and the reaction mixture was washed with water (30 ml x 4). The organic phase was dried over anhydrous magnesium sulfate ($MgSO_4$), filtered and concentrated. The crude product was purified by column chromatography on silica gel (eluents: ethyl acetate/hexane 9:1 and chloroform/methanol 8:2). Yield: 80%.

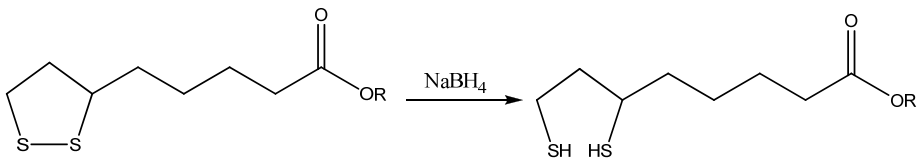

(6,8-Dimercapto-1-oxoocty)polyethylene glycol sorbitan monolaurate. Product from last step (4.96 g, 3.5 mmol) was dissolved in a mixture of EtOH/water (50 ml, 1:4). Then $NaBH_4$ (0.23 g, 6.0 mmol) was slowly added. The reaction mixture was stirred for 2 h until the solution became colorless. Then, the solution was diluted with water (50 ml) and extracted with $CHCl_3$ (50 ml) five times. The combined organic phase was dried over $MgSO_4$ and filtered. The solvent was removed under reduced pressure to give a white oily product. Yield: 81%

2.2.3.3 Preparation of water-soluble gold nanoparticles and CdSe/ZnS quantum dots

Hydrophobic nanoparticles (Au and CdSe/ZnS) (25 nmol) and DHLA-Tween20 ligand (10 μmol) were mixed in $CHCl_3$ (5 ml). The solution was stirred at room temperature for 15 minutes. Then triethylamine (0.05 ml) was added into the mixture. The resulting mixture was further stirred for 30 minutes. Equal volume of water was added into the solution. After vigorous shaking, the organic solvent was evaporated under reduced pressure to give a nanocrystal water solution. The nanocrystal solution was filtered through a 0.22-μm MCE syringe filter (Fisher Scientific). The excess of lipoic acid-Tween20 ligand was removed with centrifugal filters (Millipore, 10K NMWL, 10000×g, 30 min) for three times. The resulting nanocrystals were re-dispersed in water.

2.3 Results and Discussion

2.3.1 Ligand Synthesis

The ligand synthesis includes two steps. During the first step, lipoic acid group is added to Tween20 sturcture via a simple esterification. 4-(N,N'-Dimethylamino) pyridinium-4-toluenesulfonate (DPTS) and N,N'-diisopropyl carbodiimide (DIPC) were used to facilitate the reaction. Thin layer chromatography (TLC) is employed to monitor the reaction. The molar ratio between DPTS/DIPC and reactants will substantially affect the reaction time and yield. After the purification by column chromatography, the pure product of lipoic acid-Tween20 ester is

obtained. The structure is confirmed by ^{1}H-NMR (Figure 2-3) and 2D-NMR (Figure 2-4). Then the pure lipoic acid-Tween20 ester will be reduced by sodium borohydride to open the disulfide bond in lipoic acid. The crude product is simply purified by extraction with chloroform. Diluted HCl is added into separatory funnel to prompt the transition of reduced form from aqueous phase into chloroform. ^{1}H-NMR is shown to confirm the structure of DHLA-Tween20 (Figure 2-5).

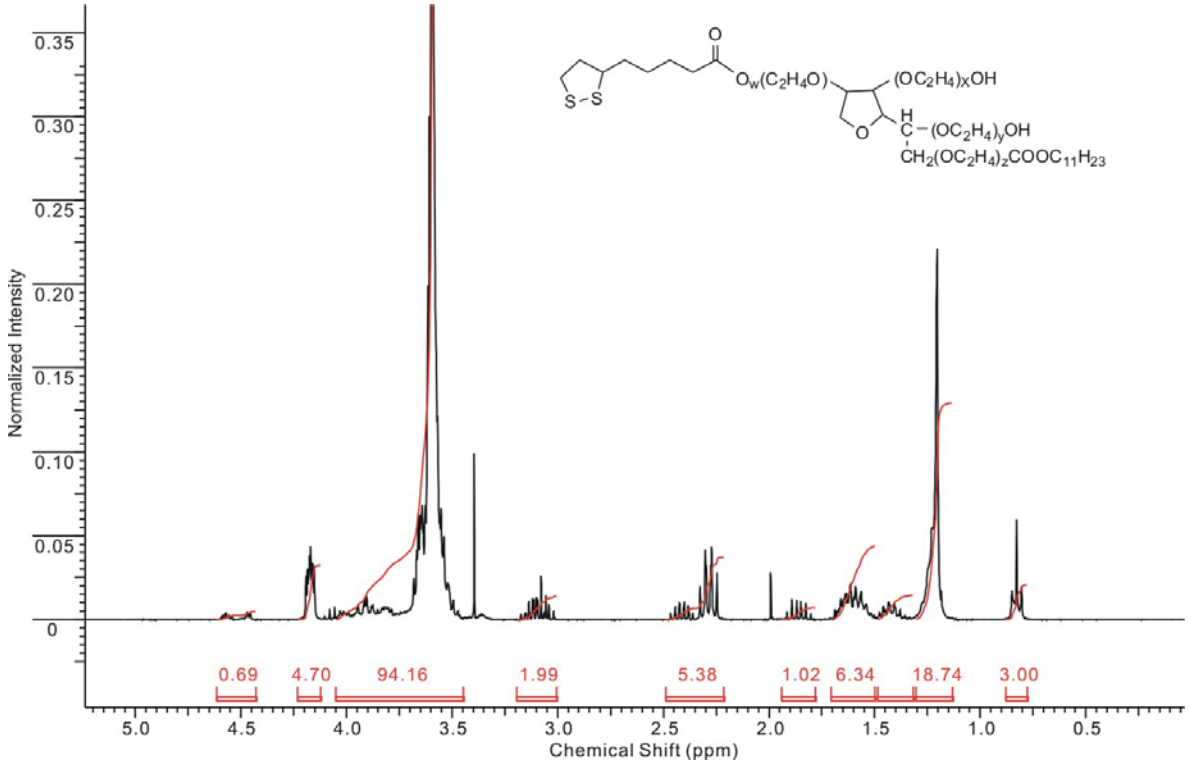

Figure 2-3. ^{1}H-NMR of lipoic acid-Tween20 ester.

2.3.2 Preparation of Water-soluble Au Nanoparticles and CdSe/ZnS QDs

The ligand exchange step is carried out in chloroform. Triethylamine is used to facilitate the ligand exchange process by increasing the basicity of the mixture. There are two different approaches to complete the phase transfer of modified nanocrystals. One can directly dry the mixture by removing the chloroform and a thin layer of nanocrystal will be left on the bottom of the vial. The nanoparticles can be re-dispersed into water to give an aqueous solution followed by purification step.

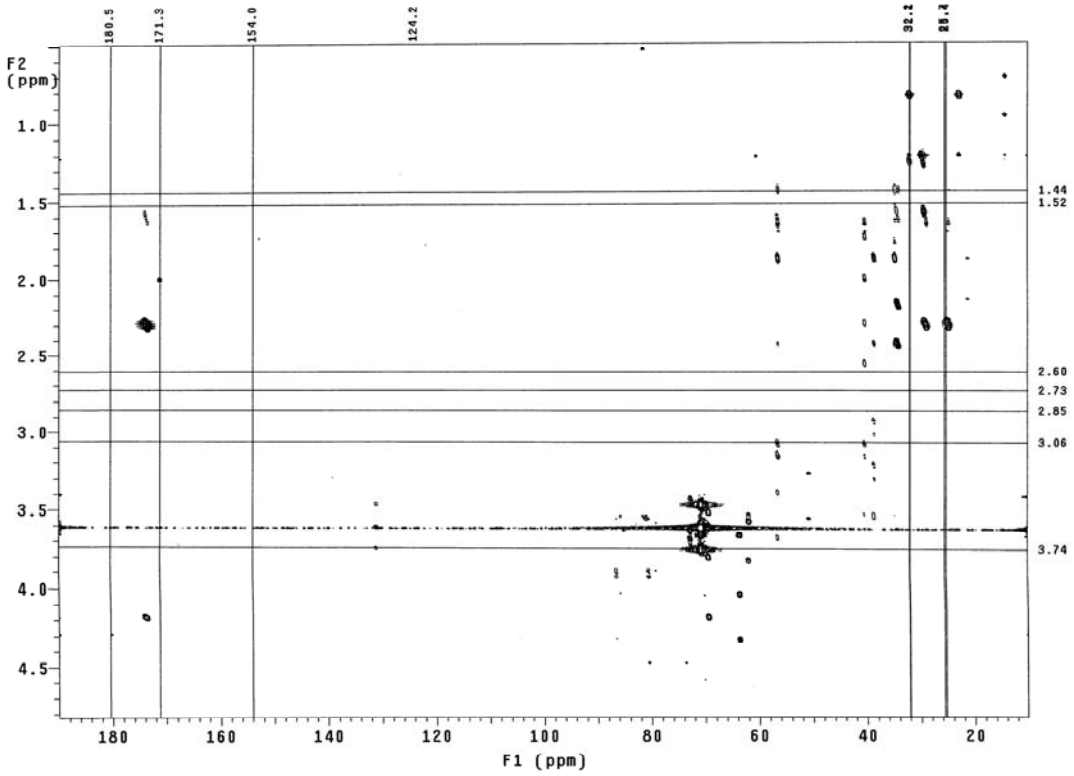

Figure 2-4. 2D-NMR of lipoic acid-Tween20 ester.

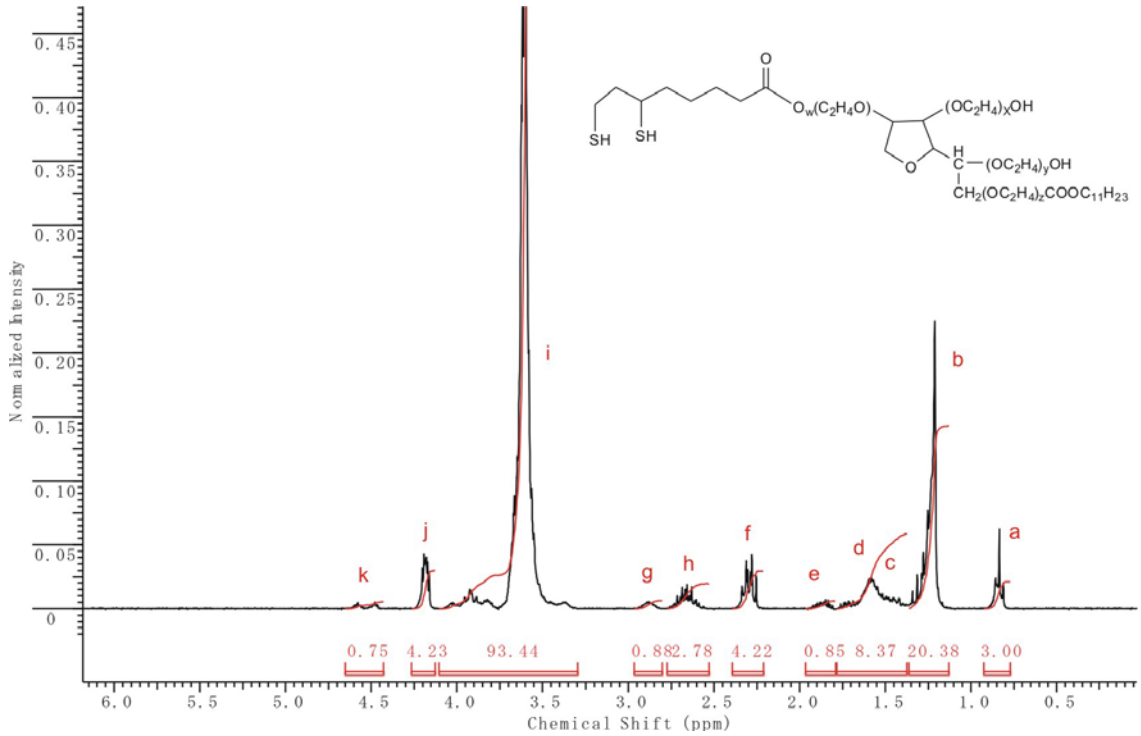

Figure 2-5. ^{1}H-NMR of DHLA-Tween20 ester.

On the contrary, in the other approach, water will be added into nanocrystal chloroform solution right after 45 minutes. Then an emulsion is made by intensively shaking the mixture. Vacuum evaporation (rotavap) will be used to remove chloroform from the mixture. Eventually, a clear nanocrystal water solution is collected. Although these two approaches seem quite similar to each other, the different phase transfer procedures could make a difference to the quality of resulting water-soluble nanocrystals. To distinguish these two methods, the quantum yields (QY) of CdSe/ZnS QDs, before and after the phase transfer using different procedure, are measured using freshly made R6G ethanol solution as fluorescence standard. The result suggests that after transferred from chloroform into water, water-soluble QDs made from rotavap-dry procedure will have 35% of QY decrease while QDs prepared with the other approach lose about 50%. Since the conformation of Tween20 in chloroform could be different than in water, the smooth transition of its conformation under rotary evaporation should result in a stronger hydrophobic interaction between the hydrophobic tail of Tween20 ligand and the remaining original ligands which will provide better protection for the inside QDs. And it could account for the difference in QY recovery between two approaches.

The obtained nanocrystals water solution needs to be further purified to remove excess free DHLA-Tween20 ligands. In searching of a better purification method, an interesting phenomenon was discovered. Because of the enhanced molecular activity, the solution containing excess DHLA-Tween20 gets turbid when it is heated to certain temperature. At which temperature (T_t) the nanoparticle solution starts to show turbidity is related to the concentration of the excess ligand in solution as suggested by UV-Vis measurement of the ligand solution (Figure 2-6). Although this measurement is not enough to quantitatively measure the amount of

excess ligand in the solution, it provides a tool to evaluate the effectiveness of the purification procedure.

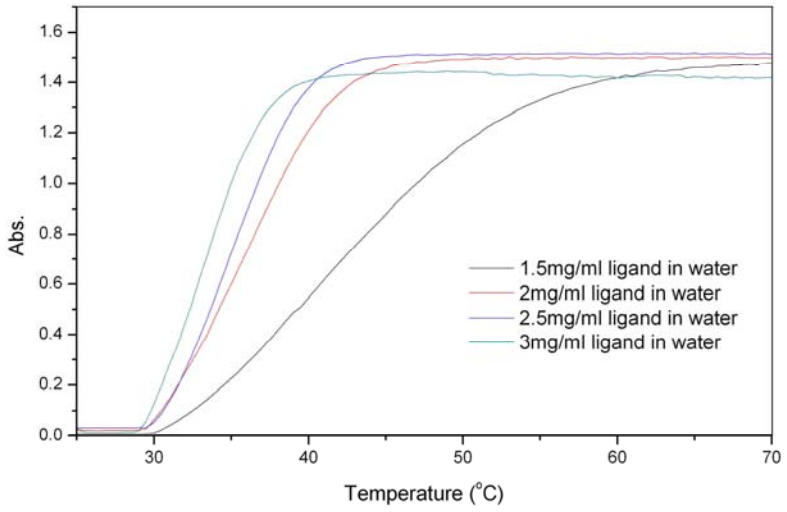

Figure 2-6. Relationship between the concentration of free ligand and the change of absorption curve.

Dialysis and centrifugal ultrafiltration are compared to select a more effective purification method. For centrifugal ultrafiltration, membrane filter with MWCO of 10,000 is used. Water-soluble nanocrystals solution is loaded into ultracentrifuge tubes with membrane filters (Figure 2-7). After 3 rounds centrifugation, the purified solution is collected. Compared to the nanocrystal solution after three day dialysis, centrifuged solution contains much less free Tween20 ligands. The result is shown in Figure 2-8.

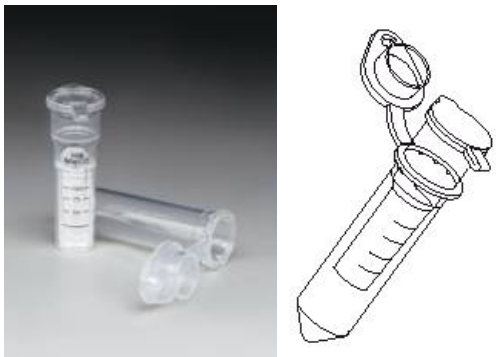

Figure 2-7. Centrifugal membrane filter unit used in nanocrystal purification.

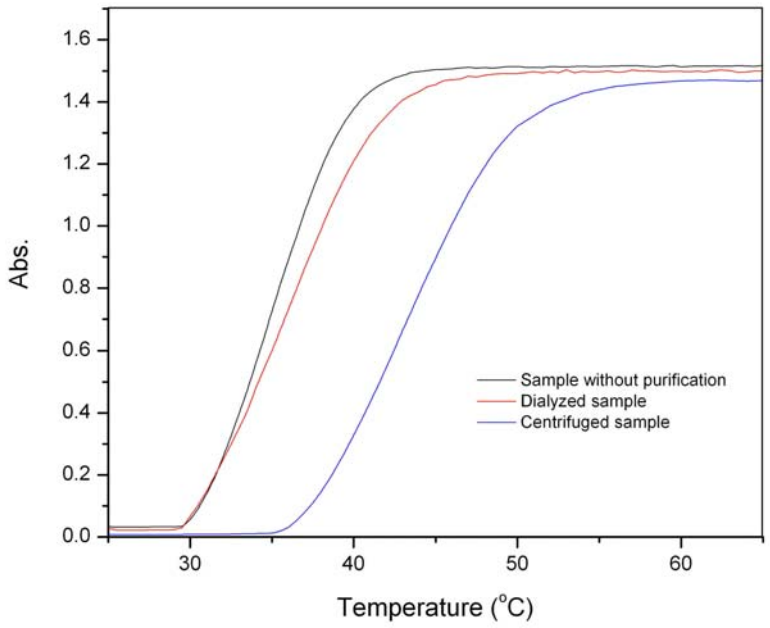

Figure 2-8. Difference in purification efficiency between dialysis and centrifugal filtration.

2.3.3 Stability

To investigate the function of the synthetic DHLA-Tween20 ligand, two types of nanocrystals, 6.6nm diameter gold nanoparticles and 5.6nm diameter CdSe/ZnS quantum dots, are selected. Transmission electron microscopy (TEM) images are shown in Figure 2-9.

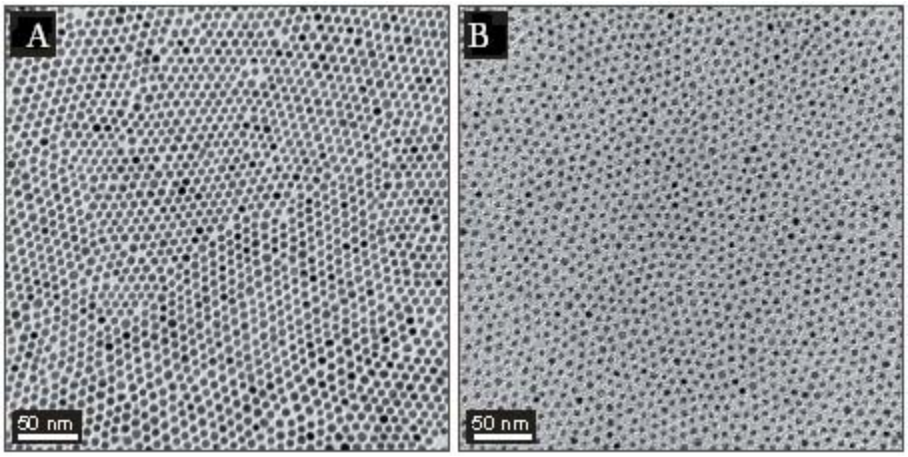

Figure 2-9. TEM images of A) Au nanoparticles and B) CdSe/ZnS QDs.

The water-soluble nanocrystals are prepared and purified following the above mentioned procedures. The hydrophilic nanocrystals are taken to TEM again. The images suggest that the modified water-soluble nanocrystals have nearly identical sizes and shapes compared to their hydrophobic counterparts (Figure 2-10).

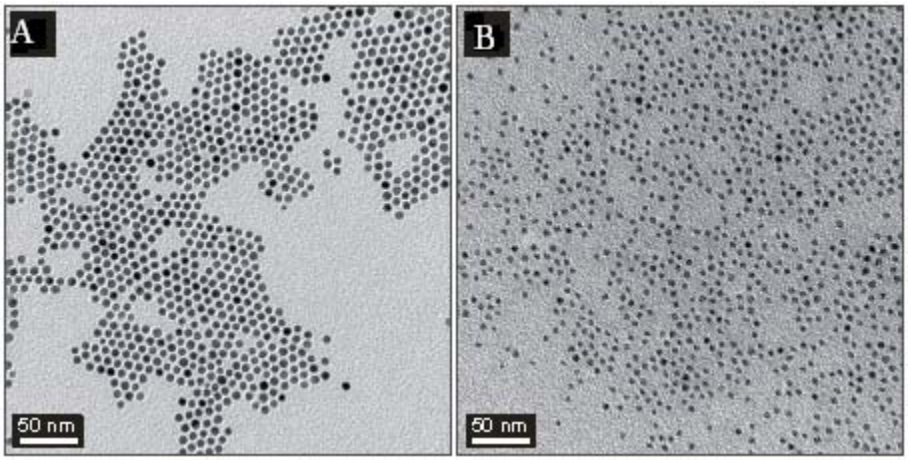

Figure 2-10. TEM images of DHLA-Tween20 functionalized A) Au nanoparticles and B) CdSe/ZnS QDs

To further understand the structure of DHLA-Tween20 functionalized nanocrystal, hydrodynamic diameters of hydrophilic gold nanoparticles and CdSe/ZnS QDs are measured by dynamic light scattering (DLS). The results show that the hydrodynamic diameters of these nanocrystals are 17.1 nm for the gold nanoparticles and 15.9 nm for the CdSe/ZnS QDs (Figure 2-11). After the subtraction of particle sizes from their hydrodynamic sizes, the average ligand shell thickness can be calculated as 5.2nm which is comparable to the average length of DHLA-Tween20 ligand (4.9nm). This result shows that there is only one layer of Tween20 ligand attached on the surface of nanocrystals.

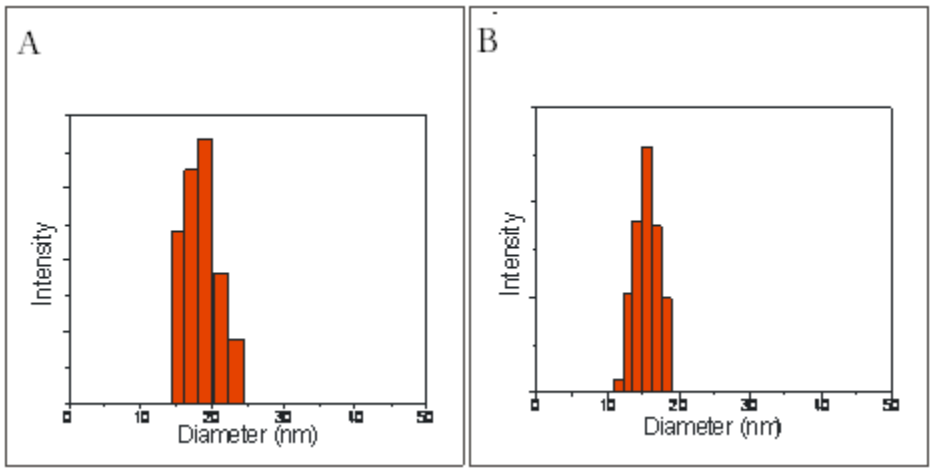

Figure 2-11. Hydrodynamic diameters of functionalized A) Au nanoparticles and B) CdSe/ZnS QDs in water solution.

Stability of DHLA-Tween20 ligand functionalized nanocrystals is tested by the measurement of absorption spectroscopy under different pH, temperature, and salt concentration. For hydrophilic gold nanoparticles, there is no change can be identified on the absorption spectra of the particles heated in boiling water for up to 4 hours (Figure 2-12).

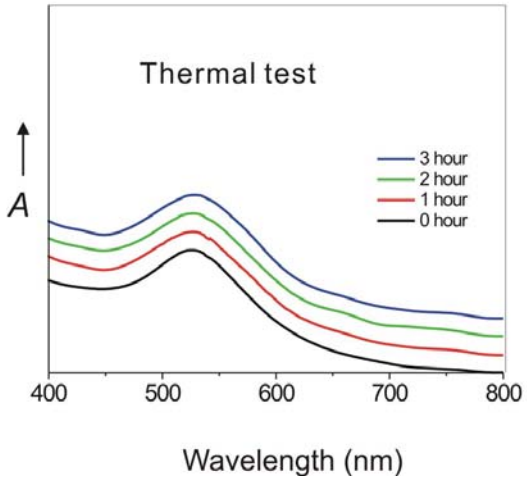

Figure 2-12. Thermal stability test of hydrophilic Au nanoparticles in boiling water.

When testing the stability as a function of pH, functionalized gold particles showed good stability at least from pH 2-13 (Figure 2-13). In addition, the gold nanoparticles are stable in NaCl solution of concentration up to 5M (Figure 2-14). Furthermore, the fluorescence quantum

yield of CdSe/ZnS in water solution is measured. It appears that after surface modification QDs still can preserve over 60% of fluorescence emission compared to the untreated hydrophobic ones. These preliminary results show the great potential of the DHLA-Tween20 ligands functionalized nanocrystals in biological applications owing to the superior stability over wide pH, temperature and salt concentration range.

Compared to the PEGylated-DHLA ligands (Figure 2-15),[60, 61] this DHLA-Tween20 ligand offers better stability under various conditions. The difference could be attributed to the hydrophobic van der Waals interaction between original surface ligands and the fatty-acid chain in Tween20, which is missing from PEGylated DHLA ligand. This hypothesis is further proved by the work done by Huimeng Wu.[62] Taken together with the results above, it shows that, in surface modification process, DHLA-Tween20 ligand presents not only coordinate bonding between its thiol groups and particle surface atoms but also a hydrophobic molecular interaction which enhances the protection to the core nanocrystal.

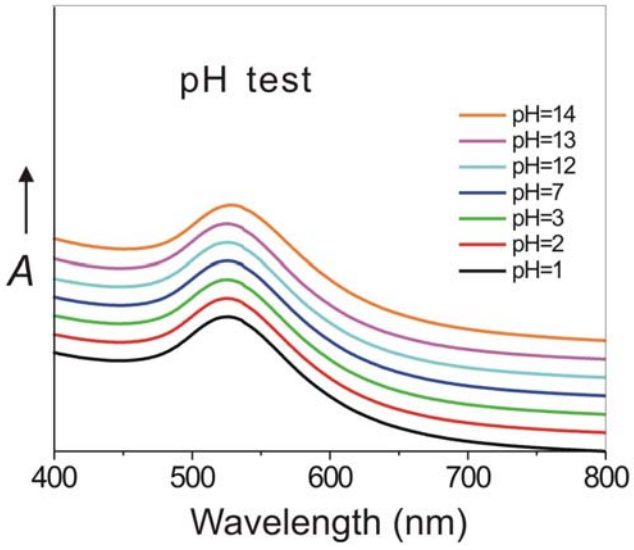

Figure 2-13. Testing Au nanoparticle stability as a function of pH.

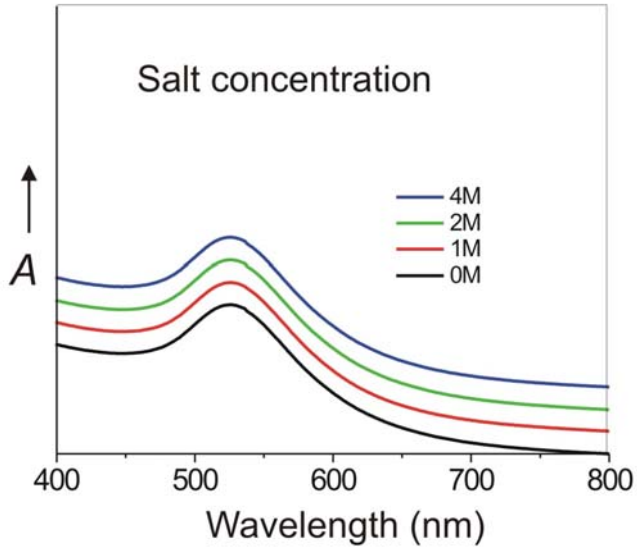

Figure 2-14. Au nanoparticle stability as a function of NaCl concentration.

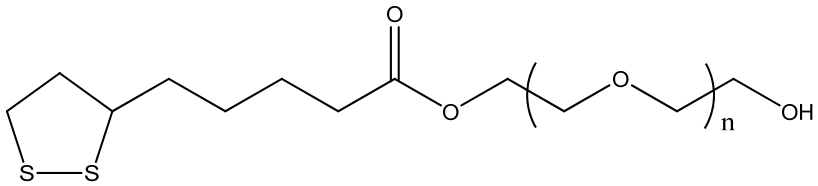

Figure 2-15. Structure of PEGylated-DHLA.

2.4 Conclusion

A dual-interaction ligand is synthesized by simple modification of Tween20 using lipoic acid. With optimized phase transfer and purification technique, high quality water-soluble gold nanoparticles and CdSe/ZnS QDs are prepared. Their stability under different conditions is tested. The results show that the DHLA-Tween20 ligand modified nanocrystals are more stable than the other water-soluble nanoparticles functionalized with either ligand exchange or polymer encapsulation approach.[3, 29, 35, 60, 61] By having both coordinate bonding and hydrophobic van der Waals interaction, this new ligand renders modified hydrophilic nanocrystals superior stability and keeps the particle size small enough to be employed into biomedical applications. This new

surface modification approach can be used to nanocrystal with different compositions and will facilitate using of nanomaterials in biological and medical research in the future.

CHAPTER 3
PREPARATION OF HYDROPHILIC GOLD NANOPARTICLES USING PHOSPHATE BASED SYNTHETIC LIGAND

3.1 Introduction

Noble metal nanoparticles, especially gold, have been extensively investigated over the past decade due to their unique electronic, optical and catalytic properties.[63, 64] These properties are different from those of bulk metal or those of molecular compounds as has been widely demonstrated in both experimental and theoretical investigations. Gold nanoparticles have a strong surface plasmon resonance in aqueous solutions, which is attributed to collective oscillations of surface electrons induced by incoming visible light. This property strongly depends on the particle size, shape and interparticle distance as well as the nature of the protecting organic shell.

During the last ten years, we witnessed the discovery of numerous applications using gold nanoparticles, especially in biomedical research. Colloidal gold particles adsorbed to antibodies or to other targeting agents, such as proteins or peptides, are widely used as labels for the detection or localization of molecular and macromolecular targets in immunoassay.[65] They can also be applied to colorimetric detection in DNA-hybridization assay as pioneered by Mirkin group in Northwestern University.[66-68] The color changes from red to blue–purple accompanying changes in the aggregation behavior have been used to detect and monitor the programming of assemblies of two and three dimensional architectures and to detect and quantify hybridization of gold nanoparticle-immobilized oligonucleotides. No matter for what purpose we are using gold nanoparticles in nanoanalytics, their properties greatly rely on their surface functionalization. Different types of ligands and surface modification approaches have been developed to extend the application using colloidal gold particles. However, in most cases, the tailoring of gold nanoparticles for a given functionality always involves the binding between two molecules, for

example, antigen–antibody, complimentary oligonucleotides, or guest–host complexes. To present biocompatibility, pre-synthesized gold nanoparticles need to be modified with new ligands or polymers having functional groups that can crosslink to certain biomolecules later. The whole process can be complicated and challenging. As an alternative, we are trying to develop a simple and straightforward method to prepare water-soluble gold nanoparticles for enzyme sensing, phosphatase in particular.

Phosphorylation and dephosphorylation play significant roles in cellular regulation and signaling processes.[69] A sensitive assay to report change of the phosphorylation state will be extremely valuable for biomedical applications. As the chemical difference in the process is only a phosphate group, a new ligand is designed (Figure 3-1). The bidentate structure possessing two thiol functional groups can make simultaneous capping attachment to two surface sites on gold nanoparticle. With the attached phosphate group, gold nanoparticle functionalized with this ligand will be well dispersed in water. However, in the presence of phosphatase which can effectively remove the phosphate group from the ligand, the gold nanoparticle will be no longer soluble in water because of the hydrophobicity of the remaining ligand. The color change and the aggregation could potentially be used to qualitatively and quantitatively detect and measuring enzyme activity.

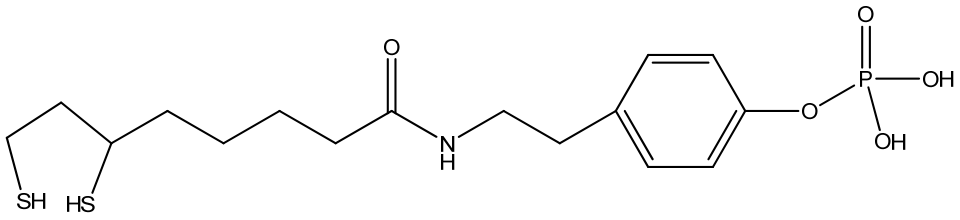

Figure 3-1. The structure of the new ligand.

In this chapter, I will focus on introducing the effort on searching an applicable approach of ligand synthesis and water-soluble particle preparation.

3.2 Experimental Section

3.2.1 Material and Instrumentation

Dimethylaminopyridine (DMAP, 99%), N,N'-diisopropyl carbodiimide (DIPC, 99%), lipoic acid (99%), tyramine (99%), diethyl phosphite (98%), bromotrimethylsilane (TMSBr, 97%)**,** sodium borohydride ($NaBH_4$, 97%), 1-dodecanethiol (97%), and p-toluenesulfonic acid monohydrate (98%), were purchased from Sigma-Aldrich. Dodecyl trimethylammonium bromide (DTAB, 97%) was purchased from Alfa Aesar. Nanopure water (18.2 MΩ·cm) was prepared by a Barnstead Nanopure Diamond system. All the other reagents and solvents were purchased from Fisher Scientific International Inc. All chemicals were used without further purification.

Absorption spectra of aliquots were collected by a Shimadzu UV-1700 UV-Visible Spectrophotometer. NMR spectra were recorded using a Varian Mercury NMR Spectrometer (300 MHz). The nanoparticle aqueous solutions were filtered through a 0.22-μm MCE syringe filter (Fisher Scientific) first and further purified with centrifugal membrane filters (Millipore, 10K NMWL).

3.2.2 Experiments

Gold nanoparticles are synthesized by following the procedure discussed in Chapter 2. 4-(N,N'-Dimethylamino)pyridinium-4-toluenesulfonate (DPTS) was prepared by mixing THF solutions of DMAP (2 M, 50 mL) and p-toluenesulfonic acid monohydrate (2 M, 50 mL) at room temperature with stirring. The resulting precipitate was filtered and dried under vacuum.

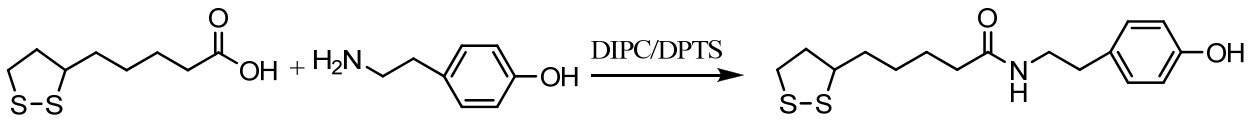

L-T: 5-(1,2-dithiolan-3-yl)-N-(4-hydroxyphenethyl)pentanamide: Lipoic acid (3.09g, 15mmol), tyramine (2.06g, 15mmol) and DPTS (5.60g, 18mmol) were dissolved into 25 ml

pyridine. Stirred for 20 min and dropwise added in DIPC (2.58ml, 18mmol). Reaction mixture was stirred overnight at room temperature. The solvent was removed under reduced pressure. The crude product was purified by column chromatography on silica gel (gradually change from ethyl acetate/hexane 3:7 to ethyl acetate/hexane 7:3). Yield: 85%.

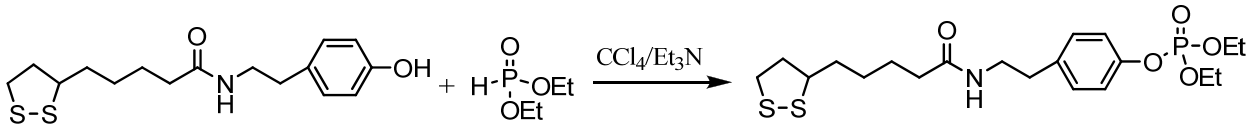

L-T-P: 4-(2-(5-(1,2-dithiolan-3-yl)pentanamido)ethyl)phenyl diethyl phosphate: 0.60 g L-T (1.8mmol) was dissolved in CCl_4/acetonitrile (10ml/5ml) with 0.50 ml diethyl phosphite (3.6mmol). The solution was cooled in ice bath. 0.50 ml triethylamine (about 3.6mmol) was added slowly into the solution with vigorous stirring. Then the mixture was warmed to room temperature and stirred overnight. The solvent was removed and the crude was dissolved in chloroform. The solution was washed with water, diluted HCl (three times), diluted NaOH (three times) and brine, successively. The organic phase was collected and dried over anhydrous magnesium sulfate ($MgSO_4$). After removing chloroform, the crude product was purified by column chromatography on silica gel (ethyl acetate/hexane 6:4, ethyl acetate/hexane 7:3 and ethyl acetate/methanol 98:2). Yield: 77%.

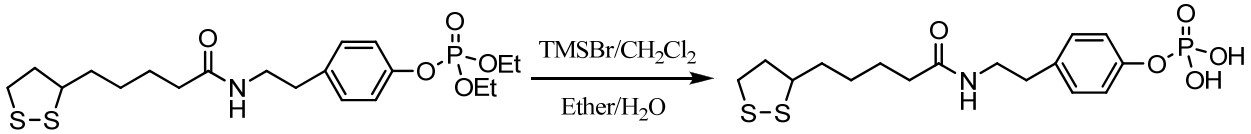

L-T-POH: 4-(2-(5-(1,2-dithiolan-3-yl)pentanamido)ethyl)phenyl dihydrogen phosphate: 0. 60g (1.3mmol) L-T-POH was dissolved in 10ml dry dichloromethane. 0.50ml of TMSBr (about 3.9mmol) was dropwise added in with vigorous stirring. The reaction solution was stirred at room temperature for three hours. TLC was used to monitor the reaction. Then diethyl ether/water (4.5ml/0.5ml) was added in. After stirring for another 10 min, product

precipitated out from the reaction mixture. Decanted and washed the crude product with diethyl ether three times. After drying under reduced pressure, product was collected. Yield: 65%.

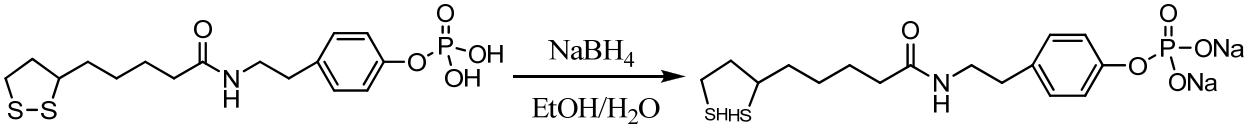

DHLA-T-P: sodium 4-(2-(6,8-dimercaptooctanamido)ethyl)phenyl phosphate. 0.330 g L-T-POH (0.8mmol) was dissolved in 3ml of ethanol/water (4:1), 0.038 g $NaBH_4$ (1mmol) was added in. The mixture was stirred under room temperature for 2 hours. Then the mixture was dried under reduced pressure. The residue was dissolved into water. This ligand-water solution was added into gold nanoparticle chloroform solution with 0.05 ml of triethylamine. The mixture was stirred for 45 minutes under room temperature. Then chloroform was removed with rotavap and the resulting gold nanoparticle aqueous solution was filtered through a 0.22-μm MCE syringe filter (Fisher Scientific). Three rounds of centrifugal filtration with centrifugal membrane filters (Millipore, 10K NMWL, 10000×g, 30 min) were carried out. The resulting nanoparticles were re-dispersed in water (Figure 3-2).

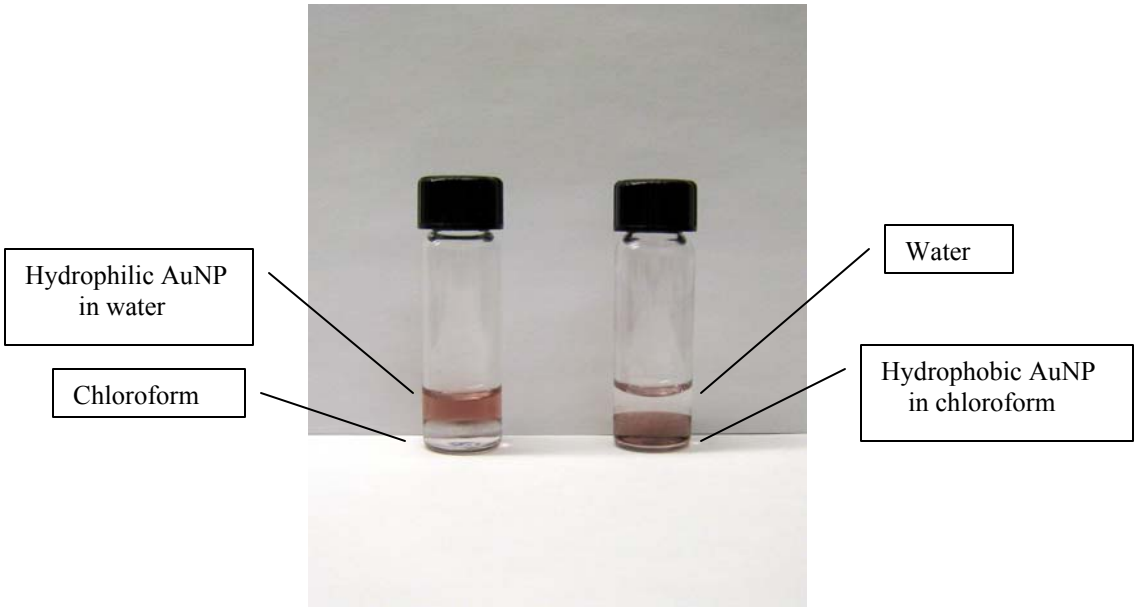

Figure 3-2. Gold nanoparticles before (right) and after (left) surface functionalization.

3.3 Results and Discussion

Phosphate-based ligands functionalized water-soluble gold nanoparticle is obtained with the following four-step synthesis route. First, a phenol group is added to lipoic acid with the formation of amide. Then a phosphate or phosphoramidite group is used to modify the structure followed by hydrolysis for making corresponding phosphoric acid. The disulfide bond can be reduced by sodium borohydride in the final step so that the resulting product will have the ability to functionalize gold nanoparticles with two free thiol groups.

For the first step, originally *N*-hydroxysuccinimide (NHS) and ethyl (dimethylaminopropyl) carbodiimide (EDC) are used to activate the carboxylic acid group in lipoic acid so that the activated carboxylic acid is able to readily react with amine group in tyramine. However, breaking esterification into two steps decreases the overall yield significantly and needs extra purification to collect desired product. To efficiently produce lipoic acid-tyramine in one step, it is critical to select an appropriate solvent that can provide resonable solubility to both lipoic acid and tyramine. After the failed experiments using dichloromethane, tetrahydrofuran (THF) and dimethylformamide (DMF), pyridine is chosen as the reaction solvent. Although the purification procedure involves more steps, the product is obtained with high reaction yield. The structure is confirmed by ^{1}H-NMR as shown in Figure 3-3.

For preparation of L-T-P, different reagents and procedures are attempted. In one procedure, 2-cyanoethyl *N*,*N*-diisopropylchlorophosphoramidite and *N*,*N*-diisopropylethylamine (DIPEA) are used to synthesize lipoic acid-tyramine phosphoramidite derivative.[70] The reaction is carried out in THF and expected to produce desired product with simple post-reaction workup. However, even with delicate column separation the pure product is still out of reach determined by proton NMR spectra (data not shown).

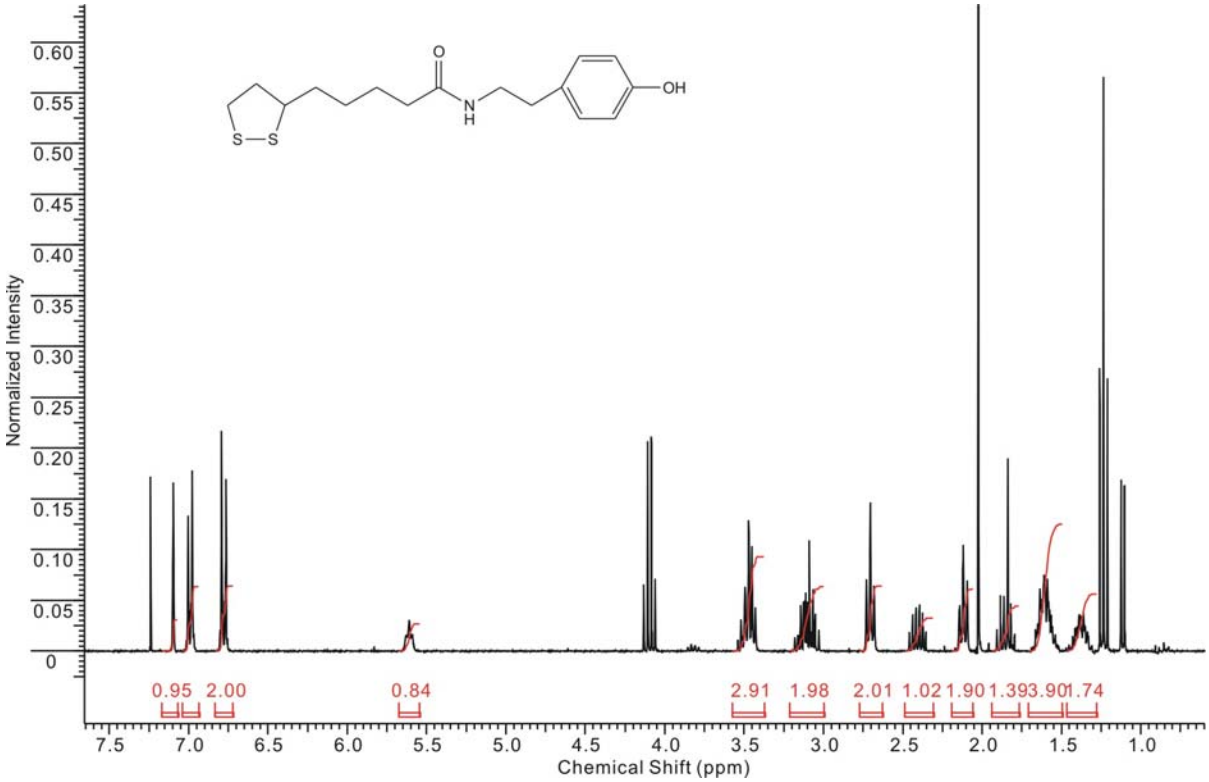

Figure 3-3. ^{1}H-NMR of lipoic acid-tyramine.

Then another more complicated synthesis procedure was adopted. It involves *in situ* silylation with tert-butylchlorodimethylsilane (TBDMSCl) followed by treatment of the silyl ester with carbon tetrachloride, diethyl phosphite and triethylamine leading to the formation of diethyl phosphoate crude product.[71] The purification process is long and difficult. During column separation, as monitored by TLC, three components are collected separately as potential product. However, neither of them can be confirmed by ^{1}H-NMR (Figure 3-4). At last, an ideal reaction system is developed by using diethyl phosphite in carbon tetrachloride/ acetonitrile mixing solvent. In this triethylamine-catalyzed reaction, acetonitrile offers good solubility to both reactants and carbon tetrachloride acts as solvent/reactant. With simple extraction and column separation, pure product is obtained in high yield and confirmed by ^{1}H-NMR, 2D-NMR and P^{31}-NMR (Figure 3-5, 6).

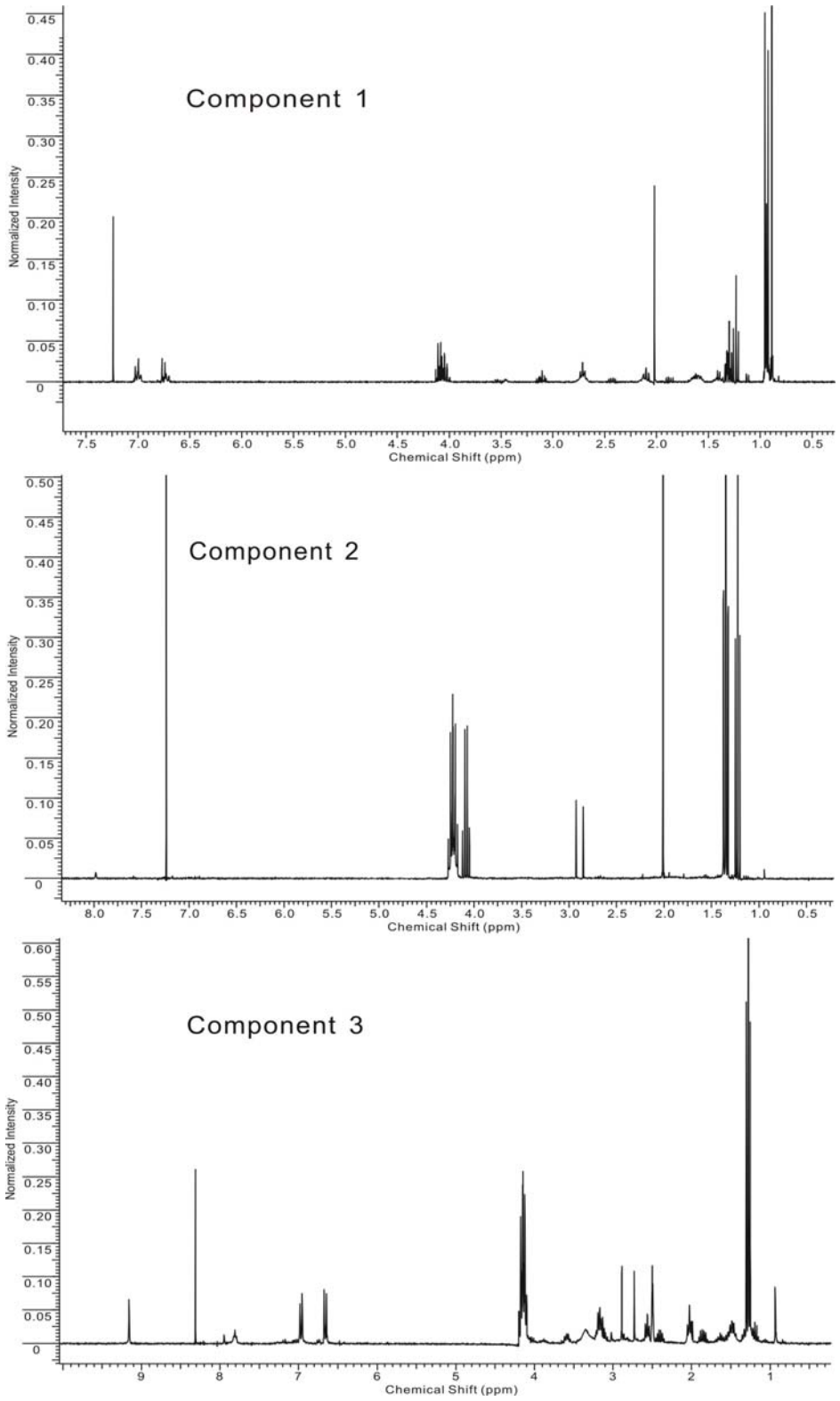

Figure 3-4. ^{1}H-NMR spectra of unidentified products in L-T-P synthesis attempt.

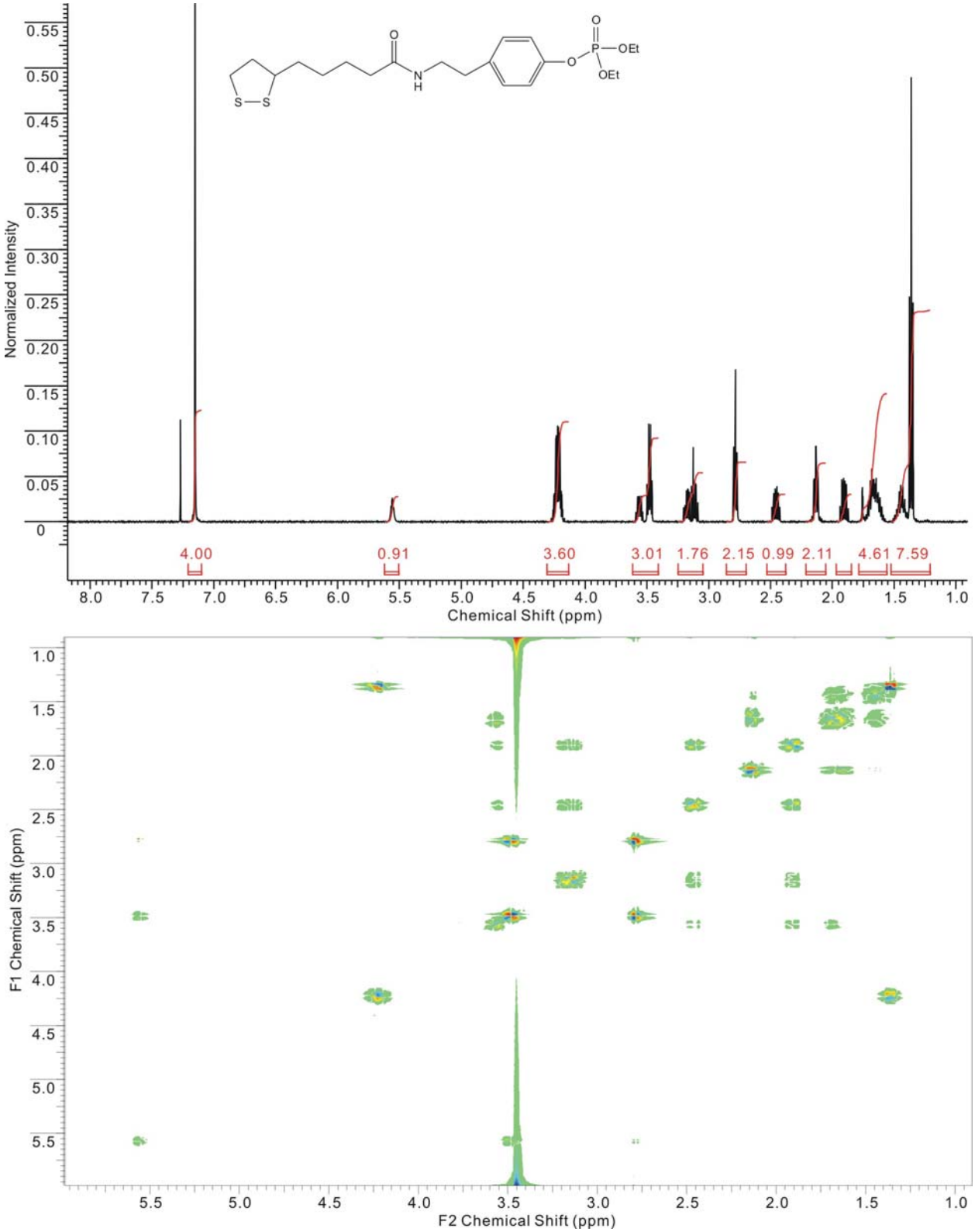

Figure 3-5. ^{1}H-NMR and 2D-NMR of L-T-P.

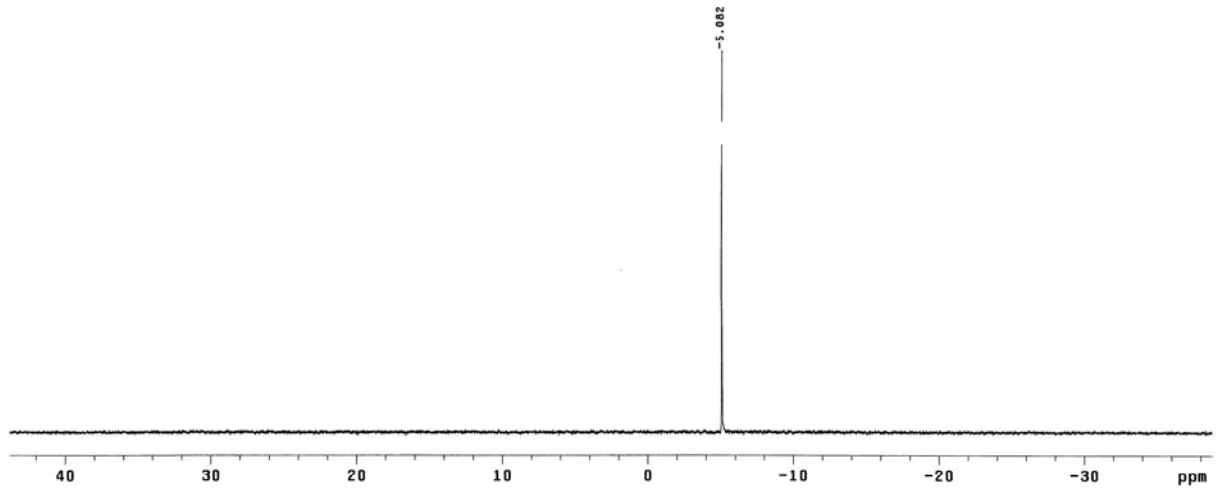

Figure 3-6. P^{31}-NMR of L-T-P.

Bromotrimethylsilane is found to be able to quantitatively convert the alkyl phosphates into the corresponding trimethylsilyl structures, which are readily transformed into the phosphoric acids by hydrolysis with neutral water.[72] By using this reagent, L-T-P is hydrolyzed to its corresponding phosphoric acid as confirmed by the only signal in P^{31}-NMR (Figure 3-7) and the absence of ethyl groups protons in ^{1}H-NMR (Figure 3-8).

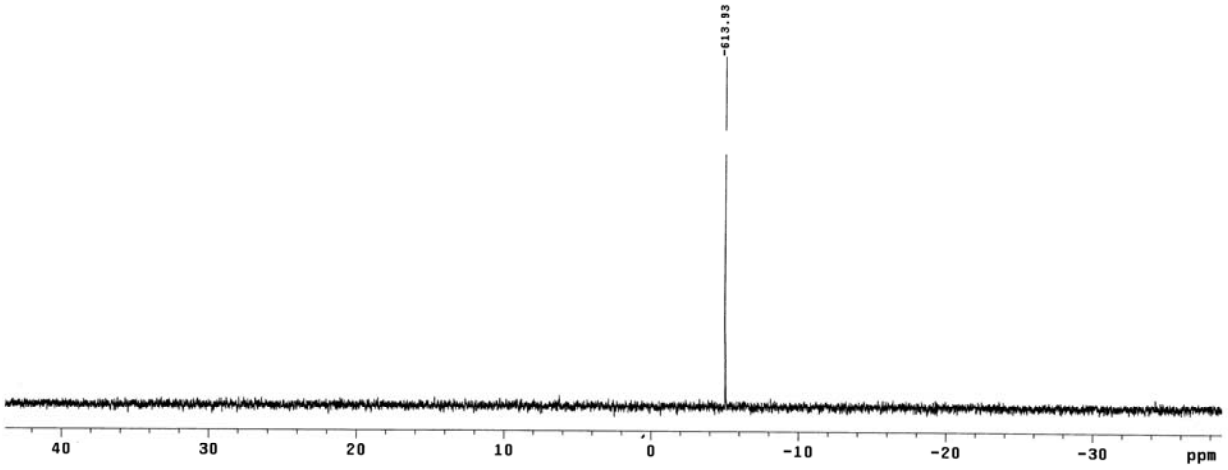

Figure 3-7. P^{31}-NMR of L-T-POH.

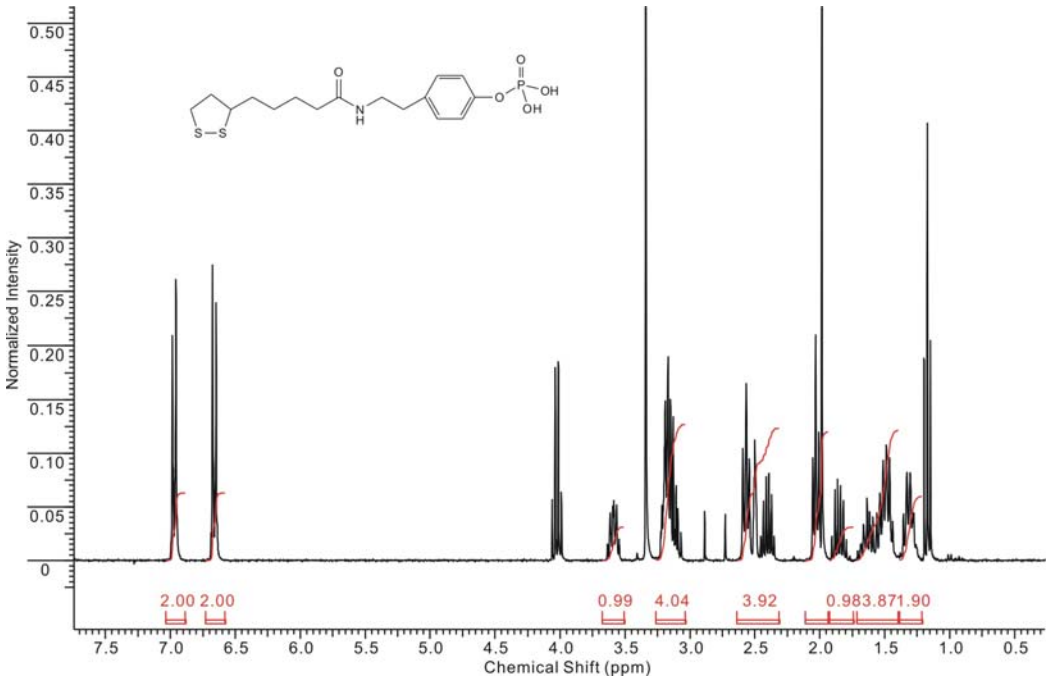

Figure 3-8. ^{1}H-NMR of L-T-POH.

The disulfide bond in resulting phosphoric acid is then reduced with sodium borohydride in 4:1 ethanol/water. Without further purification, the mixture is used to functionalize gold nanoparticle following the same procedure discussed in Chapter 2. The modified hydrophilic gold nanoparticles do not exhibit significant change in their UV-Vis absorption (Figure 3-9).

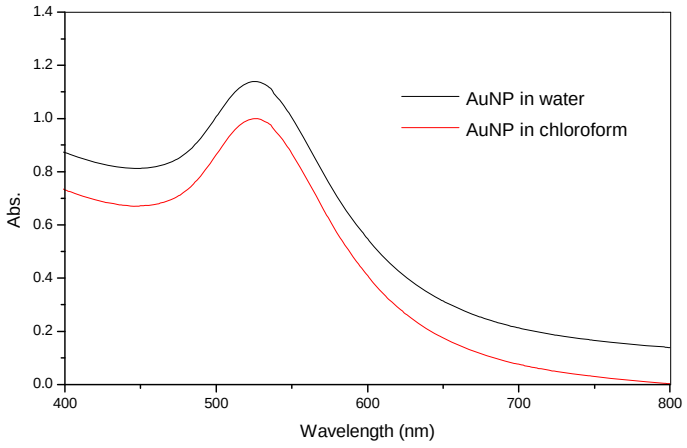

Figure 3-9. UV-Vis. absorption of AuNPs before (in chloroform) and after (in water) surface functionalization.

However, these Au nanoparticles can not survive the treatment with 0.5M NaCl solution or changing pH value of the solution. The particles will eventually aggregate and precipitate. The poor stability in aqueous solution makes it difficult to utilize these Au nanoparticles in phosphatase assay at this stage. To achieve more stable hydrophilic Au nanoparticles, it is necessary to optimize the condition of disulfide reduction step and separate pure ligand from the crude. However, it is very difficult to apply general organic separation technique such as column chromatography to this step. More work is needed in the future to improve the quality of the water-soluble particles modified by this method (please see chapter 4).

3.4 Conclusion

The experiments are partially successful as for the purpose of making phosphate based ligand functionalized hydrophilic gold nanoparticles. The modified gold nanoparticles show basically no change in their UV-Vis absorption in water. However, because of the imperfection of the final reduction step, the stability of the modified particles is relatively low which make it difficult to carry on the phosphatase assay at this stage. To obtain high quality water-soluble Au nanoparticles, it is necessary to separate the final product from the crude mixture and optimize the surface functionalization procedure.

CHAPTER 4
SUMMARY AND FUTURE WORK

4.1 Summary

It has been demonstrated that, with design and synthesis of different organic ligands, hydrophobic nanocrystals can be transferred into hydrophilic ones and functionalized for various applications, especially in biological and medical studies. The interaction between synthetic ligands and nanocrystal surface can be categorized into two major types: coordinate binding and hydrophobic molecular interaction. Ligands can be anchored on the surface of the particle by using one or both of these two types of interaction. The new ligands are also expected to deliver desired biocompatibility to the nanocrystal. Normally, one class of synthetic ligands is specifically related to one class of biomolecules as determined by the nature of specific recognition in biological system, such as DNA hybridization, antigen-antibody, peptides and proteins. To be employed in biomedical applications, one or more of the following four properties of hydrophilic nanocrystals will be needed: good solubility and distribution; sufficient chemical stability; appropriate particle size; and high quantum yield for QDs.

It was proved that a dual-interaction ligand can be synthesized by simply using lipoic acid and Tween20 polymer. With the optimized surface functionalization technique, the modified hydrophilic nanocrystals are well dispersed in water and stable under different pH, temperature and salt concentration. At the same time, these nanocrystals have a smaller hydrodynamic size compared to those of polymer encapsulated nanoparticles. This surface modification approach, using both coordinate bonding and hydrophobic molecular interaction, will facilitate the application of nanocrystals in biological labeling, targeting, imaging and sensing.

In the other part of my work, another lipoic acid based ligand was synthesized. Hydrophilic gold nanoparticle was obtained by the surface functionalization using this phosphate

ligand. However, the modified Au nanoparticle is not very stable in its aqueous solution. This may result from the imperfection of the last step in ligand synthesis. To be used in phosphatase detection, the synthesis and surface modification procedure need to be optimized.

4.2 Future Work

Quantum dots have been extensively used in biological applications because of their unique properties. But they are limited in lots of applications due to either low chemical stability or oversize dimension after surface functionalization. Lipoic acid-Tween ligands have been proved for their superior stability and good biocompatibility.[62] Using this new class of ligands to modify quantum dots may produce more opportunities for their biological applications. One can functionalize magnetic/luminescent bifunctional nanocrystals with lipoic acid-Tween ligand and target them to particular *in vivo* sites, such as tumors, and make novel magnetic resonance imaging agents. Also they can be used for deep-tissue imaging which needs good permeability and long-term stability in biological environment. Another interesting area involves QDs' extensive multiplexing detection potential which hasn't been fully utilized. Using lipoic acid-Tween ligand to protect and functionalize QDs for a multiplex labeling system can be exciting and may alter the view of in vivo labeling and imaging.

For using water-soluble gold nanoparticle for phosphatase sensing, more stable particles are needed. To get pure ligand in the last step, other separation techniques can be used, such as HPLC or immobilized reducing agent gel column. Tris(2-carboxyethyl)phosphine (TCEP) serves as excellent agent for the reduction of disulfide bonds in proteins, peptides and other disulfide bond-containing molecules and are relatively unreactive toward other functional groups.[75, 76] Immobilized TCEP disulfide reducing gel column may be useful in reducing disulfide in the synthetic ligand without introducing any impurity. If more stable hydrophilic gold nanoparticle

can be obtained, it is promising that we will be able to develop an assay for simple and rapid phosphatase detection.

LIST OF REFERENCES

1. Murray, C.B.; Norris, D.J; Bawendi, M.G. *J. Am. Chem. Soc.* **1993**, *115*, 8706-8715.

2. Coe, S.; Woo, W.-K.; Bawendi, M. G.; Bulovic, V. *Nature* **2002**, *420*, 800-803.

3. Gao, X.; Cui, Y.; Levenson, R. M.; Chuang, L.W.K.; Nie, S. *Nat. Biotechnol.* **2004**, *22*, 969-976.

4. Huynh, W.U.; Dittmer, J.J.; Alivisatos, A.P. *Science* **2002**, *295*, 2425-2427.

5. Cao, Y.; Bannin, U. *J. Am. Chem. Soc.* **2000**, *122*, 9692-9702.

6. Battaglia, D.; Peng, X. *Nano Lett.* **2002**, *2*, 1027-1030.

7. Yu, M.W.; Peng, X. Angew. *Chem., Int. Ed.* **2002**, *41*, 2368-2371.

8. Jun, Y. W.; Lee, S. M.; Kang, N. J.; Cheon, J. *J. Am. Chem. Soc.* **2001**,*123*, 5150-5151.

9. Joo, J.; Na, H.B.; Yu, T.; Yu, J.H.; Kim, Y.W.; Wu, F.X.; Zhang, J.Z.; Hyeon, T. *J. Am. Chem. Soc.* **2003**, *125*, 11100-11105.

10. Lee, S. M.; Jun. Y.W.; Cho, S.N.; Cheon, J. *J. Am. Chem. Soc.* **2002**,*124*,11244-11245.

11. Hines, M.A.; Scholes, G.D. *Adv. Mater.* **2003**,*15*,1844-1849.

12. Alivisatos, A. P. *Nat. Biotechnol.* **2004**, *22*, 47-52.

13. Han, M.; Gao, X.; Su, J.Z.; Nie, S. *Nat. Biotechnol.* **2001**, *19*, 631-635.

14. Bruchez, M. Jr.; Moronne, M.; Gin, P.; Weiss, S.; Alivisatos, A.P. *Science* **1998**, *281*, 2013-2016.

15. Chan, W.C.; Nie, S. *Science*, **1998**, *281*, 2016-2018.

16. Alivisatos, A. P. *J. Phys. Chem. B* **1996**, *100*, 13226-13239.

17. Alivisatos, A. P. *Science* **1996**, *271*, 933-937.

18. Murray, C. B.; Kagan, C. R.; Bawendi, M. G. *Annu. Re*V. *Mater. Sci.* **2000**, *30*, 545-610.

19. Peng, Z. A.; Peng, X. *J. Am. Chem. Soc.* **2001**, *123*, 183-184.

20. Peng, Z. A.; Peng, X. *J. Am. Chem. Soc.* **2002**, 124, 3343-3353.

21. Peng, X.; Dchlamp, M.C.; Kadavanich, A.V.; Alivisatos, A.P. *J. Am. Chem. Soc.* **1997**,*119*, 7019-7029.

22. Mekis, I.; Talapin, D.V.; Kornowski, A.; Haase, M.; Well, H. *J. Phys. Chem. B* **2003**, *107*, 7454-7462.

23. Aldana, J.; Wang, Y. A.; Peng, X. *J. Am. Chem. Soc.* **2001**, *123*, 8844-8850.

24. Hines, M. A.; Guyot-Sionnest, P. *J. Phys. Chem.* **1996**, *100*, 468-471.

25. Yu, W.W.; Chang, E.; Drezek R.; Colvin, V.L. *Biochem. Biophys. Res. Commum*. **2006**, 348, 781–786.

26. Mattoussi, H.; Mauro, J.M.; Goldman, E.R.; Anderson, G.P.; Sundar, V.C.; Mikulec, F.V.; and Bawendi, M.G. *J. Am. Chem. Soc.* **2000**, 122**,** 12142–12150.

27. Mitchell, G. P.; Mirkin, C. A; Letsinger, R. L. *J. Am. Chem. Soc.* **1999**, 121**,** 8122–8123.

28. Goldman, E. R.; Balighian, E. D.; Mattoussi, H.; Kuno, M.K.; Mauro, J. M.; Tran, P.T.; Anderson, G. P. *J. Am. Chem. Soc.* **2002**, 124**,** 6378–6382.

29. Uyeda, H. T.; Medintz, I, L.; Jaiswal, J. K.; Simon, S. M.; Mattoussi H. *J. Am. Chem. Soc.* **2005,** 127, 3870–3878.

30. Pathak, S.; Choi, S.K.; Arnheim, N.; Thompson, M.E. *J. Am. Chem. Soc.* **2001,** 123, 4103**–**4104.

31. Kim, S.; Bawendi, M.G. *J. Am. Chem. Soc.* **2003**, 125, 14652**–**14653.

32. Pinaud, F.; King, D.; Moore, H.P.; Weiss, S. *J. Am. Chem. Soc*. **2004**, 126, 6115**–**6123.

33. Guo, W.; Li, J.J.; Wang, Y.A.; Peng, X. *Chem. Mater*. **2003**, 15, 3125**–**3133.

34. Dubertret, B.; Skourides, P.; Norris, D.J.; Noireaux, V.; Brivanlou, A.H.; Libchaber, A. *Science* **2002**, 298, 1759–1762.

35. Yu, W.W.; Chang, E.; Falkner, J.C.; Zhang, J.; Al-Somali, A.M.; Sayes, C.M.; Johns, J.; Drezek, R.; Colvin, V.L. *J. Am. Chem. Soc.* **2007**, 129, 2871 -2879.

36. Gerion, D.; Pinaud, F.; Williams, S.C.; Parak, W.J.; Zanchet, D.; Weiss, S.; Alivisatos, A.P. *J. Phys. Chem.* **2001**, 105, 8861**–**8871.

37. Nann, T.; Mulvaney, P. *Angew. Chem. Int. Ed.* **2004**, 43, 5393**–**5396.

38. Selvan, S.T.; Bullen, C.; Ashokkumar, M.; Mulvaney, P. *Adv. Mater*. **2001**, 13, 985**–**988.

39. Rogach, A.L.; Nagesha, D.; Ostrander, J.W.; Giersig, M.; Kotov, N.A. *Chem. Mater.* **2000**, 12, 2676**–**2685.

40. Miyawaki, A. *Dev. Cell* **2003**, 4**,** 295–305.

41. Leatherdale, C. A.; Woo, W. K.; Mikulec, F. V.; Bawendi, M. G. *J. Phys. Chem. B.* **2002**, 106, 7619–7622.

42. Parak, W. J. *et al. Nanotech.* **2003**, 14, R15–R27.

43. Niemeyer, C. M. *Angew. Chem. Int. Edn Eng.* **2001**, 40, 4128–4158.

44. Medintz, I.L.; Uyeda, H.T.; Goldman, E.R.; Mattoussi, H. *Nat. Mater.* **2005**, 4, 435 – 446.

45. Jaiswal, J. K.; Mattoussi, H.; Mauro, J. M.; Simon, S. *Nature Biotechnol.* **2003**, 21**,** 47–51.

46. Chen, F.; Gerion, D. *Nano Lett.* **2004**, 4, 1827–1832.

47. Derfus, A. M.; Chan, W. C. W.; Bhatia, S. N. *Adv. Mater.* **2004**, 16**,** 961–966.

48. Voura, E. B.; Jaiswal, J. K.; Mattoussi, H.; Simon, S. M. *Nature Med.* **2004**, 10, 993–998.

49. Larson, D.R.; Zipfel, W.R.; Williams, R.M.; Clark, S.W.; Bruchez, M.P.; Wise, F.W.; Webb. W.W. *Science* **2003**, 300**,** 1434–1437.

50. Michalet, X.; Pinaud, F.F.; Bentolila, L.A.; Tsay, J.M.; Doose, S.; Li, J.J.; Sundaresan, G.; Wu, A.M.; Gambhir, S.S.; Weiss, S. *Science* **2005**, 307, 538 – 544.

51. Xu, C.; Xu, K.; Gu, H.; Zheng, R.; Liu, H.; Zhang, X.; Guo, Z.; Xu, B. *J. Am. Chem. Soc.* **2004**, 126, 9938 – 9939.

52. Xie, J.; Xu, C.; Xu, Z.; Hou, Y.; Young, K.L.; Wang, S.X.; Pourmand, N.; Sun, S. *Chem. Mater.* **2006**, 18, 5401 – 5403.

53. Fan, H.; Leve, E.W.; Scullin, C.; Gabaldon, J.; Tallant, D.; Bunge, S.; Boyle, T.; Wilson, M.C.; Brinker, C.J. *Nano Lett.* **2005**, 5, 645 – 648.

54. Wu, X.; Liu, H.; Liu, J.; Haley, K.N.; Treadway, J.A.; Larson, J.P.; Ge, N.; Peale, F.; Bruchez, M.P. *Nat. Biotechnol*. **2003**, 21, 41 – 46.

55. Smith, A.M.; Duan, H.; Rhyner, M.N.; Ruan, G.; Nie, S. *Phys. Chem. Chem. Phys.* **2006**, 8, 3895 – 3903.

56. Garti, N. *Lebensm.-Wiss. Technol.* **1997**, 30, 222 – 235.

57. Burnette, W.N. *Anal. Biochem.* **1981**, 112, 195 – 203.

58. Engvall, E.; Perlman, *P. Immunochemistry* **1971**, 8, 871 – 874.

59. Shevchenko, E.V.; Talapin, D.V.; Kotov, N.A.; O'Brien S.; Murray, C.B. *Nature* **2006**, 439, 55.

60. Liu, W.H.; Howarth, M.; Greytak, A.B.; Zheng, Y.; Nocera, D.G.; Ting, A.Y.; Bawendi, M.G. *J. Am. Chem. Soc.* **2008**, 130, 1274 –1284.

61. Susumu, K.; Uyeda, H.T.; Medintz, I.L.; Pons, T.; Delehanty, J.B.; Mattoussi, H. *J. Am. Chem. Soc.* **2007**, 129, 13987 – 13996.

62. Wu, H.; Zhu, H.; Zhuang, J.; Yang, S.; Liu, C.; and Cao, Y.C. *Angew. Chem. Int. Ed.* **2008**, 47, 3730 -3734.

63. Kreibig, U.; Vollmer, M. *Optical Properties of Metal Clusters*, Springer, Berlin, 1995.

64. Daniel, M.C.; Astruc, D. *Chem. Rev.*, **2004**, 104, 293–346.

65. Krisch, B.; Feindt, J.; and Mentlein, R. *J. Histochem. Cytochem.* **1998**, 46, 1233–1242.

66. Elghanian, R.; Storhoff, J.J.; Mucic, R.C.; Letsinger, R.L.; and Mirkin, C.A. *Science,* **1997**, 277, 1078–1081.

67. Niemeyer, C.M.; and Mirkin, C.A. *Nanobiotechnology: Concepts, Applications and Perspectives*. **2004**.

68. Park, S.J.; Taton, T.A.; and Mirkin, C.A. *Science*, **2002**, 295, 1503–1506.

69. Kennelly, P.J. *Chem. Rev*. **2001**, 101(8).

70. Letsinger, R.L.; Elghanian, E.; Viswanadham, G.; Mirkin, C.A. *Bioconjugate Chem.* **2000**, 11 (2), 289 -291.

71. Szardenings, A.K.; Gordeev, M.F.; Patel, D.V. *Tetra. Lett.* **1996**, 37, 3635-3638.

72. McKenna, C.E.; Schmidhauser, J. *J. C. S. Chem. Comm.* **1979**, 739.

73. Kim, S. *et al. Nature Biotechnol.* **2004**, 22, 93–97.

74. Ballou, B.; Lagerholm, B.C.; Ernst, L.A.; Bruchez, M.P.; Waggoner, A.S. *Bioconj. Chem.* **2004**, 15, 79–86.

75. Ruegg, U.T.; Rudinger, J. *Methods Enzymol.* **1977**, 47, 111-126.

76. Kirley, T.L. *Anal. Biochem.* **1989**, 180, 231.

BIOGRAPHICAL SKETCH

Shuo Yang was born in Beijing, China in 1978. He spent the first seven years of his life in Shanxi province and moved to Tianjin with his parents in 1985. After spending almost ten years in Tianjin, the family moved back to Beijing in1995. He started his college life at the Peking University Health Science Center and graduated with bachelor's degree in science four years later. Before he came to the Department of Chemistry in 2005, he received another master's degree from Department of Medicinal Chemistry in College of Pharmacy at the University of Florida. He would like to continue his study and pursue a Ph.D. degree in the near future.